J. Fluid Mech. (1994), *vol.* 274, *pp.* 163–195

Hypersonic boundary-layer separation on a cold wall

By R. M. KERIMBEKOV[1], A. I. RUBAN[1] AND J. D. A. WALKER[2]

[1] Central Aerohydrodynamic Institute, Zhukovsky-3, Moscow Region, 140160, Russia

[2] Department of Mechanical Engineering and Mechanics, Lehigh University, Bethlehem, Pennsylvania 18015, USA

(Received 13 July 1992 and in revised form 28 February 1994)

An asymptotic theory of laminar hypersonic boundary-layer separation for large Reynolds number is described for situations when the surface temperature is small compared with the stagnation temperature of the inviscid external gas flow. The interactive boundary-layer structure near separation is described by well-known triple-deck concepts but, in contrast to the usual situation, the displacement thickness associated with the viscous sublayer is too small to influence the external pressure distribution (to leading order) for sufficiently small wall temperature. The present interaction takes place between the main part of the boundary layer and the external flow and may be described as inviscid–inviscid. The flow in the viscous sublayer is governed by the classical boundary-layer equations and the solution develops a singularity at the separation point. A main objective of this study is to show how the singularity may be removed in different circumstances.

1. Introduction

The first crucial insight into separation phenomena at high Reynolds numbers was provided by Prandtl (1904) who argued that fluid motion is reduced to relative rest on solid walls within thin viscous boundary layers where the kinetic energy of fluid particles is considerably reduced. The flow near the surface is therefore very sensitive to streamwise pressure variations and, as a consequence, rapid deceleration and flow reversal can be induced by even a small pressure rise. In such situations, a recirculation zone can form near the wall, and for steady flow past a stationary wall, the skin friction changes sign along the body contour, with the point of zero skin friction usually referred to as the separation point. According to the Prandtl classical interactive strategy, the fluid motion around a rigid body is to be evaluated via a hierarchal scheme in which: (i) a solution of the Euler equations for the external flow problem produces an estimate of pressure distribution along the body surface, and (ii) the boundary-layer solution is evaluated using this pressure distribution. The displacement effect of the boundary layer can then be computed and the external inviscid solution is refined in an obvious iteration. Unfortunately, the classical interactive strategy fails in most circumstances (Smith 1982) because a singularity is encountered in the boundary-layer solution at the separation point $x = x_s$, in any situation where the pressure gradient is prescribed. Landau & Lifschitz (1944) described the structure of this singularity, showing that at locations upstream of x_s, the skin friction decreases proportional to $(x_s - x)^{1/2}$, while the slope of the streamlines diverges proportional to $(x_s - x)^{-1/2}$. A crucial result was later obtained by Goldstein (1948) who demonstrated that the solution of the boundary-layer equations cannot be continued downstream of x_s. This

is an apparent contradiction since, as Stewartson (1970) has pointed out, there is no obvious reason why reversed flow downstream of x_s 'cannot be accommodated in the thin boundary layer'.

The first theoretical studies that resolved this apparent paradox were based on investigations of a 'free' or 'self-induced' interaction, originally observed experimentally by Chapman, Kuehn & Larsen (1958). In the experiments, an oblique shock wave incident on a flat-plate boundary layer was observed to provoke separation well upstream of the point of intersection of the shock wave and the boundary layer. However, since the boundary-layer equations are parabolic, disturbances cannot be transmitted upstream within the boundary layer and the observed 'upstream influence' induced by the shock wave can only be described in terms of a solution structure which is locally interactive with the external flow. A theoretical framework for free interaction problems was constructed by Neiland (1969), Stewartson & Williams (1969), Messiter (1970) and Sychev (1972) through asymptotic analysis of the Navier–Stokes equations in the limit of Reynolds number $Re \to \infty$. A three-layer interaction region was shown to exist in the vicinity of the separation point having a streamwise extent $O(Re^{-3/8})$ and consisting of: (i) a thin near-wall viscous sublayer having a thickness $O(Re^{-5/8})$; (ii) a middle layer having a thickness $O(Re^{-1/2})$, corresponding to that of the upstream boundary layer; and (iii) an upper layer of thickness $O(Re^{-3/8})$, occupying a portion of the external flow above the boundary layer. Since the velocities in the viscous sublayer are small, this region is very susceptible to pressure variations, and even a slight pressure rise $O(Re^{-1/4})$ is sufficient to provoke a nonlinear response and reversed flow. The middle region is essentially a continuation of the upstream boundary layer where the flow is essentially inviscid and only slightly disturbed; for this reason the contribution to the displacement thickness associated with the middle region is usually negligible compared with that of the sublayer. In the upper layer, the flow is inviscid and governed by linearized compressible flow equations.

The motion in the viscous sublayer is governed by the usual Prandtl boundary-layer equations. However, the pressure $p(x)$ is not known in advance, and is related through an interaction law to the displacement function $A(x)$ associated with the sublayer. This relation is either the Ackeret law or a Cauchy integral relation, namely

$$p(x) = -\frac{\mathrm{d}A}{\mathrm{d}x}, \quad p(x) = \frac{1}{\pi}\int_{-\infty}^{\infty} \frac{\mathrm{d}A/\mathrm{d}s}{x-s}\,\mathrm{d}s, \tag{1.1 a, b}$$

for either a supersonic or a subsonic external flow, respectively. The functions $A(x)$ and $p(x)$ must generally be found through an iterative solution of the boundary-layer equations and one of the interaction laws (1.1).

The boundary-layer solution is generally initiated upstream from the condition

$$u \to y \quad A(x) \to 0 \quad \text{as} \quad x \to -\infty, \tag{1.2}$$

and it follows that the scaled viscous stress $\tau = \partial u/\partial y \to 1$ as $x \to -\infty$. Consequently, the skin friction τ_w is positive, and it follows that the interaction region of interest must be located well upstream of the Goldstein singularity at x_s. Stewartson (1970) studied another alternative to condition (1.2) involving an interaction region surrounding a Goldstein singularity at x_s, but was able to demonstrate that there is no solution to such a problem for either of the interaction laws (1.1). Thus the Goldstein singularity is not removable and separation cannot be explained in terms of a gradual deceleration of the boundary layer over an $O(1)$ distance along the wall under the influence of an adverse pressure gradient. In fact, at least in the context of separation regions that are

confined within the dimensions of the viscous sublayer, separation occurs as a result of an abrupt self-induced pressure rise within the interaction region. Solutions containing regions of reversed flow may be obtained which do not exhibit a singular behaviour at the separation point. However, it is necessary generally to formulate an additional condition as $x \to \infty$, which reflects the fact that the interaction region merges into a known flow downstream. Such a condition affects the solution of the interaction problem, even for an unseparated supersonic boundary layer (Lighthill 1953). In any event, it is clear that the propagation of disturbances upstream observed by Chapman *et al.* (1958) can be explained in terms of a local interaction between the external flow and the boundary layer. Interaction theory has subsequently been applied to a great number of separation problems as reviewed by Neiland (1974, 1981), Stewartson (1974, 1981), Lagerstrom (1975), Messiter (1979, 1983), Adamson & Messiter (1980), Smith (1982) and in the recent monograph of V. Sychev *et al.* (1987).

The present paper is concerned with hypersonic boundary-layer separation on a cold wall. The problem was first considered by Neiland (1973) who showed that: (i) cooling of the wall leads to a decrease in displacement thickness of the viscous sublayer, and (ii) the contribution due to the main part of the boundary layer $\Delta\delta^*$ is proportional to the induced pressure rise according to $\Delta\delta^* = \mathscr{L}p$, where $\mathscr{L}$ is given by

$$\mathscr{L} = \int_0^{\delta} \left(\frac{1}{M^2} - 1 \right) \mathrm{d}Y. \tag{1.3}$$

This integral first appeared in a study of high-speed injection into a nozzle (Pearson, Holliday & Smith 1958); here δ denotes boundary-layer thickness and $M(Y)$ is the Mach number distribution across the boundary layer. The influence of the main part of the boundary layer depends on the sign of $\mathscr{L}$. If the average Mach number is less than unity, $\mathscr{L} > 0$ and a pressure increase leads to boundary-layer thickening, as in the case of a subsonic mainstream. On the other hand if $\mathscr{L} < 0$, a pressure rise produces a decrease in boundary-layer thickness as is usual for a supersonic mainstream. Consequently, a boundary layer with $\mathscr{L} > 0$ is termed subcritical and that with $\mathscr{L} < 0$ is referred to as supercritical. For a cold wall, the conventional Ackeret law (equation (1.1*a*)) must be modified (Neiland 1973) to the form

$$p(x) = S\mathscr{L}\frac{\mathrm{d}p}{\mathrm{d}x} - \frac{\mathrm{d}A}{\mathrm{d}x}. \tag{1.4}$$

The terms on the right-hand side of (1.4) are associated with contributions to displacement thickness due to the main part of the boundary layer and the viscous sublayer, respectively. Here S is a parameter that will be formally defined in §2, which depends on the Mach and Reynolds numbers and varies inversely with respect to wall temperature. In normal circumstances S is small and (1.4) reduces to the conventional Ackeret formula. On the other hand, when the wall temperature is small with respect to the stagnation temperature of the external mainstream flow, S may be $O(1)$ or $S \gg 1$. The situation where S is large is of interest in this study where the first term in (1.4) is dominant and for which an inviscid–inviscid interaction occurs between the external flow and the main part of the boundary layer. In this case, the analysis of the viscous sublayer must be carried out in the context of a prescribed pressure gradient and under certain circumstances the solutions develop a singularity at the separation point. However, because the singularity is already embedded within an interactive structure, it is not removable by the methods discussed by Neiland (1969), Stewartson & Williams (1969), Messiter (1970) and Sychev (1972).

Hypersonic flows with strong wall cooling are of considerable current interest owing to the necessity of maintaining the thermal integrity of future hypersonic vehicles (Walberg 1991; Townend 1991). In general, complex multi-layer phenomena can occur in this environment, especially when boundary-layer separation develops; recently Messiter, Matarrese & Adamson (1991) have studied the case of strip blowing on a wedge and Brown, Cheng & Lee (1990) have investigated compressive free interactions and the compression ramp with strong wall cooling. The present study is also concerned with the compression ramp and the relation to the work of Brown *et al.* (1990) will be discussed subsequently. The problem is formulated in §2, and the supercritical and subcritical cases are addressed in §3 and §4 respectively. The nature and type of singularities encountered and how they may be removed is discussed in each case.

2. Formulation

2.1. *The upstream boundary layer*

Consider the flow of an ideal gas past the solid body shown in figure 1, consisting of a plate of length L oriented parallel to a uniform flow upstream, with a second plate inclined at ramp angle θ. The upstream flow has speed U_∞, density ρ_∞, enthalpy h_∞ and pressure p_∞, and the specific heat ratio γ is assumed constant. Define flow variables such that lengths, velocities, pressure, density, enthalpy and absolute viscosity are made dimensionless with respect to L, U_∞, p_∞, ρ_∞, U_∞^2 and μ_0 respectively; here μ_0 is the viscosity coefficient evaluated at a reference enthalpy of U_∞^2, which is appropriate for large Mach number. The viscosity coefficient μ' is assumed to depend on the temperature alone according to the power law $\mu' = (h')^n$, where n is a positive constant and h' is the enthalpy; the prime will be used throughout to denote unscaled non-dimensional variables. The Reynolds number and mainstream Mach number are defined by

$$Re_0 = \rho_\infty U_\infty L/\mu_0, \quad M_\infty = U_\infty(\gamma p_\infty/\rho_\infty)^{-1/2}, \tag{2.1a, b}$$

and both are assumed to be large. The analysis is presented in terms of two parameters, namely the hypersonic viscous interaction parameter χ and ϵ defined by

$$\chi = M_\infty^2 Re_0^{-1/2}, \quad \epsilon = Re_0^{-1/4}, \tag{2.2}$$

both of which are small. Note that Re_0 is defined in terms of μ_0; a Reynolds number Re based on μ_∞ (evaluated at the mainstream static temperature) may also be defined (Brown *et al.* 1990), and for $n = 1$, Re is proportional to $M_\infty^2 Re_0$.

As shown in figure 1, Cartesian coordinates (x', y'), with origin at the leading edge of the first plate, are adopted with corresponding velocity components (u', v'). Scaled boundary-layer variables upstream of the corner are defined by

$$y' = \epsilon\chi^{1/2}Y, \quad v' = \epsilon\chi^{1/2}V(x', Y)+\ldots, \quad p' = 1+\chi P(x', Y)+\ldots,$$
$$\rho' = M_\infty^{-2}R(x', Y)+\ldots, \tag{2.3a–d}$$

where p' and ρ' are the pressure and density respectively. Substitution into the Navier–Stokes equations yields

$$Ru'\frac{\partial u'}{\partial x'}+RV\frac{\partial u'}{\partial Y} = \frac{\partial}{\partial Y}\left(\mu'\frac{\partial u'}{\partial Y}\right), \quad \frac{\partial(Ru')}{\partial x'}+\frac{\partial(RV)}{\partial Y} = 0, \tag{2.4a, b}$$

$$Ru'\frac{\partial h'}{\partial x'}+RV\frac{\partial h'}{\partial Y} = \frac{1}{Pr}\frac{\partial}{\partial Y}\left(\mu'\frac{\partial h'}{\partial Y}\right)+\mu'\left(\frac{\partial u'}{\partial Y}\right)^2, \tag{2.4c}$$

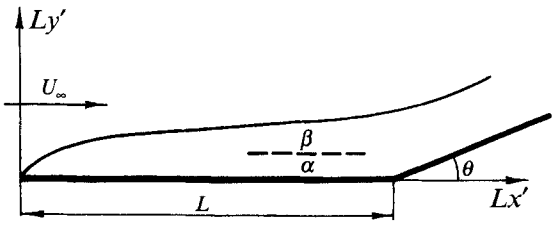

FIGURE 1. Geometry and coordinate system.

where u', h' and μ' are functions of (x', Y), and the Prandtl number Pr is assumed constant. The viscosity law and ideal-gas state equation are

$$\mu' = (h')^n, \quad h' = \frac{1}{(\gamma-1)R}, \tag{2.5a, b}$$

respectively. The mainstream enthalpy (non-dimensionalized by U_∞^2) is $O(M_\infty^{-2})$ as $M_\infty \to \infty$ and thus the matching conditions to the mainstream require

$$u' \to 1, \quad h' \to 0 \quad \text{as} \quad Y \to \delta(X), \tag{2.6}$$

where $\delta(X)$ denotes the boundary-layer thickness. At the plate surface,

$$u' = V = 0, \quad h' = g_w = h_w^*/U_\infty^2 \quad \text{at} \quad Y = 0, \tag{2.7a–c}$$

where h_w^* is the dimensional wall enthalpy and g_w is called the temperature factor. Commonly, g_w is $O(1)$, such as for an adiabatic wall or some specified surface temperature distribution. However, in this study the wall is cold in the sense that $g_w \ll 1$; this condition implies that the surface temperature T_w is small with respect to the stagnation temperature of the external inviscid flow but not necessarily that $T_w \ll T_\infty$, where T_∞ is the mainstream static temperature. In view of the viscous dissipation term in (2.4c), h' is $O(1)$ in the boundary layer, and thus for $g_w \ll 1$, $h' = 0$ to leading order at the wall; it is now shown that in this circumstance the upstream boundary layer splits into two regions, denoted α and β in figure 1.

One possible solution of the upstream equations (2.4) has a self-similar form in which u', h' and R are functions of $\eta = Y(x')^{-1/2}$, but this special form is not required in the subsequent analysis. In fact, the theory may be applied to a variety of body configurations (other than in figure 1), where a hypersonic boundary layer approaches a compression corner, even if the surface temperature is not constant. For the following development, it is only essential that the dimensionless shear stress ($\mu' \partial u'/\partial Y$) and heat flux ($\mu' Pr^{-1} \partial h'/\partial Y$) are $O(1)$ as $Y \to 0$. It follows, using the viscosity law (2.5a), that the asymptotic solution of (2.4) may be expressed as

$$u' \to a(x')\, Y^{1/(n+1)}, \quad h' \to b(x')\, Y^{1/(n+1)}, \quad R \to \frac{Y^{-1/(n+1)}}{(\gamma-1)\, b(x')} \quad \text{as} \quad Y \to 0. \tag{2.8a–c}$$

Here the arbitrary functions $a(x')$ and $b(x')$ can, in principle, be obtained from a 'global' solution of (2.4), taking into account all boundary conditions.

It is easily inferred from (2.8) that the solution is not uniformly valid near the wall since the density function $R \to \infty$ as $Y \to 0$. Although h' tends to zero for small Y, a new region must be considered near the wall having a thickness such that $Y^{1/(n+1)} = O(g_w)$ in order to satisfy the exact condition (2.7c). This inner zone is denoted region α in

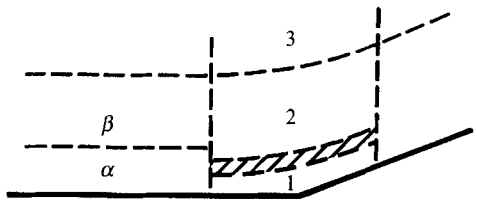

FIGURE 2. Schematic diagram of the multilayer structure that develops near the corner (not to scale).

figure 1, with the main part of the boundary layer being region β. It follows from (2.3) and (2.8) that in the near-wall region α

$$u' = g_w \hat{u}(x', \hat{Y}) + \ldots, \quad v' = \epsilon\chi^{1/2} g_w^{n+2} \hat{V}(x', \hat{Y}) + \ldots, \quad y' = \epsilon\chi^{1/2} g_w^{n+1} \hat{Y}, \tag{2.9a–c}$$

$$h' = g_w \hat{h}(x', \hat{Y}) + \ldots, \quad \rho' = M_\infty^{-2} g_w^{-1} \hat{R}(x', \hat{Y}) + \ldots, \quad \mu' = g_w^n \hat{\mu}(x', \hat{Y}) + \ldots, \tag{2.9d–f}$$

where p' is described by (2.3c) and $\hat{Y}$ is $O(1)$ in zone α. Substitution of (2.9) into the Navier–Stokes equations shows that the viscous and conduction terms are dominant in the momentum and energy equations, namely

$$\frac{\partial}{\partial \hat{Y}}\left(\hat{\mu}\frac{\partial \hat{u}}{\partial \hat{Y}}\right) = 0, \quad \frac{\partial}{\partial \hat{Y}}\left(\hat{\mu}\frac{\partial \hat{h}}{\partial \hat{Y}}\right) = 0, \tag{2.10a, b}$$

to leading order and (2.5) becomes $\hat{\mu} = \hat{h}^n$, $\hat{h} = (\gamma - 1)^{-1} \hat{R}^{-1}$. The solution of (2.10) satisfying $\hat{u} = \hat{V} = 0$, $\hat{h} = 1$ at $\hat{Y} = 0$ and which matches with the solution (2.8) in region β as $\hat{Y} \to \infty$ has the form

$$\hat{u} = \frac{a(x')}{b(x')}\{[b(x')]^{n+1}\hat{Y} + 1\}^{1/(n+1)} - \frac{a(x')}{b(x')}, \quad \hat{h} = \{[b(x')]^{n+1}\hat{Y} + 1\}^{1/(n+1)}. \tag{2.11a, b}$$

In particular,

$$\hat{u} \to \frac{a(x')[b(x')]^n}{n+1}\hat{Y} + \ldots, \quad \hat{\mu}, \hat{h} \to 1 + \ldots, \quad \text{as} \quad \hat{Y} \to 0. \tag{2.12a–c}$$

2.2. *Estimates for the interaction region*

A multi-layer structure occurs in the corner shown in figure 2 and here physical arguments will be used first to establish the relevant orders of magnitude. Suppose (subject to verification) that a viscous sublayer (labelled region 1 in figure 2) occurs in the interaction region, which is much thinner than the upstream sublayer α. The following estimate for the streamwise velocity component in region 1 is suggested from matching with the solution (2.9a, c) and (2.12a) in region α:

$$u' \sim y'/(\epsilon\chi^{1/2} g_w^n). \tag{2.13}$$

Here y' is synonymous with the thickness of region 1 and $\sim$ is used throughout this section to imply comparable magnitude. When the pressure rise $\Delta p'$ induced by the interaction is sufficiently large to provoke a nonlinear response in the sublayer 1 (figure 2), the velocity variation $\Delta u'$ is comparable to u'. Taking into account the non-dimensionalizations introduced in §2.1 and (2.1), a balance between the inertia terms and each of the pressure gradient and viscous terms gives

$$g_w^{-1}(u')^2 \sim \Delta p', \quad g_w^{-1} M_\infty^{-2} \frac{(u')^2}{\Delta x'} \sim Re_0^{-1} g_w^n \frac{u'}{(y')^2}, \tag{2.14a, b}$$

respectively. Here the density estimate $\rho' \sim M_\infty^{-2} g_w^{-1}$ has been used (from (2.9*e*)) and $\Delta x'$ denotes the longitudinal extent of the interaction region. A further relation follows from linearized compressible flow theory describing the external pressure disturbance induced by the displacement effect of the sublayer; this is the Ackeret formula which in the present dimensionless variables gives

$$\Delta p' \sim M_\infty y'/\Delta x'. \tag{2.15}$$

Equations (2.13)–(2.15) may be solved for u', $\Delta p'$, y' and $\Delta x'$ to yield

$$\Delta x' \sim \chi^{3/4} g_w^{n+1/2}, \quad y' \sim \epsilon\chi^{3/4} g_w^{n+1/2}, \quad u' \sim \chi^{1/4} g_w^{1/2}, \quad \Delta p' \sim \chi^{1/2}. \tag{2.16a–d}$$

The estimates (2.16) are valid provided the contribution to the displacement thickness associated with the main part of the boundary layer (region 2 in figure 2) is at most comparable with that of sublayer 1. To assess the contribution of region 2, note that here $u' \sim 1$, $\rho' \sim M_\infty^{-2}$ and $p' \sim 1$ in order to merge to the upstream layer β described by (2.3); in addition, the effectively inviscid flow is isentropic satisfying $p'(\rho')^{-\gamma} = \text{constant}$. Consequently, it is easily shown that along each streamline in region 2

$$\Delta u' \sim \Delta p', \quad \Delta\rho' \sim \rho' \Delta p', \tag{2.17a, b}$$

from the streamwise momentum equation and isentropic relation, respectively. It follows from (2.16*d*) and (2.17) that the flow perturbations in region 2 are linear since $\chi \ll 1$, in contrast to the nonlinear response produced in region 1 (cf. (2.14*a*)). Furthermore, if d denotes the normal distance between any two streamlines in region 2, it is easily shown from continuity of mass that $\Delta d \sim d\Delta p'$, where from (2.3*a*) d is $O(\epsilon\chi^{1/2})$; consequently, using equation (2.16*d*), it is evident that $\Delta d \sim \epsilon\chi$, and thus the lateral separation distance Δd of two arbitrary streamlines is small with respect to any initial value d.

Consider now the most general flow regime (Neiland 1973) when regions 1 and 2 both contribute to the displacement thickness so that $\Delta d \sim y'$. It is easily shown using (2.16*b*) that this regime occurs for g_w small and specifically

$$g_w^{n+1/2} \sim \chi^{1/4}. \tag{2.18}$$

It may be verified that the thickness of region 1 is g_w^n times smaller than the near-wall layer α upstream, while the extent $\Delta x'$ of the interaction region is $O(M_\infty)$ larger than the upstream boundary-layer thickness. Consequently, the normal pressure variation across regions 1 and 2 is expected to be negligible to leading order.

2.3. *Formulation of the interaction problem*

From the estimates (2.16), scaled variables in sublayer 1 are defined by

$$(x'-1, y') = \chi^{3/4} g_w^{n+1/2}(x^*, \epsilon y^*), \quad (u', v') = \chi^{1/4} g_w^{1/2}(u^*, \epsilon v^*) + \ldots, \tag{2.19a–d}$$

$$p' = 1 + \gamma\chi^{1/2} p^* + \ldots, \quad h' = g_w h^* + \ldots, \quad \rho' = M_\infty^{-2} g_w^{-1} \rho^* + \ldots, \quad \mu' = g_w^n \mu^* + \ldots. \tag{2.19e–h}$$

Substitution of (2.19) into the Navier–Stokes and energy equations shows that $\partial p^*/\partial y^* = 0$, $h^* = \mu^* = 1$ and $\rho^* = 1/(\gamma-1)$, respectively, the latter results following from matching to equations (2.12) in region α. Therefore, the flow in the sublayer 1 is incompressible to leading order and the governing equations are

$$\frac{1}{\gamma-1}\left(u^* \frac{\partial u^*}{\partial x^*} + v^* \frac{\partial u^*}{\partial y^*}\right) = -\frac{dp^*}{dx^*} + \frac{\partial^2 u^*}{\partial y^{*2}}, \quad \frac{\partial u^*}{\partial x^*} + \frac{\partial v^*}{\partial y^*} = 0. \tag{2.20}$$

The velocities u^* and v^* must vanish at the body contour $y^* = Y_0^*(x^*)$ defined by

$$Y_0^*(x^*) = 0 \quad \text{if} \quad x^* < 0; \quad Y_0^* = \theta_0 x^* \quad \text{if} \quad x^* > 0. \tag{2.21}$$

Here the ramp angle is defined by $\theta = \epsilon\theta_0$, where θ_0 is assumed to be an $O(1)$ constant.

To match the solution (2.12) in the upstream region α,

$$u^* \to \lambda y^* + \ldots \quad \text{as} \quad x^* \to -\infty, \quad \lambda = ab^n/(n+1). \tag{2.22}$$

Here a and b denote the limiting values of $a(x')$ and $b(x')$ as $x \to 1$, which are obtainable from a global solution of (2.4) in the upstream boundary layer. For finite x^*, the solution of (2.20) must have the following asymptotic form:

$$u^* \to \lambda y^* + \lambda A^*(x^*) + \ldots, \quad v^* \to -\lambda \frac{\mathrm{d}A^*}{\mathrm{d}x^*} y^* + \ldots \quad \text{as} \quad y^* \to \infty, \tag{2.23}$$

where $A^*(x^*)$ is a displacement function, which is to be found from a solution of the complete interaction problem.

The next zone is an intermediate layer between regions 1 and 2 (shown in figure 2 as the hatched area), which is a continuation of the upstream near-wall region α. The normal variable $\hat{Y}$ in region α is related to y^* by $\hat{Y} = g_w^{-1/2} \chi^{1/4} y^*$; substitution in the asymptotic form (2.23), using (2.19*c*, *d*), gives

$$u' = \lambda g_w \hat{Y} + \lambda g_w^{1/2} \chi^{1/4} A^*(x^*) + \ldots, \quad v' = \epsilon g_w \left(-\lambda \frac{\mathrm{d}A^*}{\mathrm{d}x^*} \right) \hat{Y} + \ldots, \tag{2.24a, b}$$

and this suggests the following expansions in the intermediate layer:

$$(u', h') = g_w \{\hat{U}_0(\hat{Y}), \hat{H}_0(\hat{Y})\} + g_w^{1/2} \chi^{1/4} \{\hat{U}_1, \hat{H}_1\} + \ldots, \quad v' = \epsilon g_w \hat{V}_1 + \ldots, \tag{2.25a–c}$$

where the functions $\hat{U}_1$, $\hat{H}_1$, and $\hat{V}_1$ are functions of $(x^*, \hat{Y})$. The expansion for pressure is given by (2.19*e*) and

$$\rho' = M_\infty^{-2} \{g_w^{-1} \hat{R}_0(\hat{Y}) + g_w^{-3/2} \chi^{1/4} \hat{R}_1(x^*, \hat{Y}) + \ldots\}, \quad \mu' = g_w^n \hat{\mu}_0(\hat{Y}) + \ldots. \tag{2.26a, b}$$

Upon substitution in the Navier–Stokes equations, it is easily shown that the solution matching that in the sublayer 1 as $\hat{Y} \to 0$ is given by

$$\hat{U}_0(\hat{Y}) = (a/b)\{\hat{H}_0(\hat{Y}) - 1\}, \quad \hat{H}_0(\hat{Y}) = \{b^{n+1} \hat{Y} + 1\}^{1/(n+1)}, \tag{2.27a, b}$$

with $\hat{\mu}_0 = \hat{H}_0^n$ and $\hat{R}_0 = (\gamma - 1)^{-1} \hat{H}_0^{-1}$. Consequently, the leading terms in (2.25) are simply the continuation of the solution in region α into the interaction zone. The matching conditions to the sublayer $\hat{U}_1 \to \lambda A^*$ and $\hat{V}_1 \to -\lambda(\mathrm{d}A^*/\mathrm{d}x^*)\hat{Y}$ as $\hat{Y} \to 0$ follow from (2.24), and it is easily shown that

$$\hat{U}_1 = A^*(x^*) \frac{\mathrm{d}\hat{U}_0}{\mathrm{d}\hat{Y}}, \quad \hat{V}_1 = -\frac{\mathrm{d}A^*}{\mathrm{d}x^*} \hat{U}_0(\hat{Y}), \quad \hat{H}_1 = A^*(x^*) \frac{\mathrm{d}\hat{H}_0}{\mathrm{d}\hat{Y}}. \tag{2.28a–c}$$

It may be inferred from (2.25) and (2.28) that the slope of the streamlines is invariant across the intermediate region and is given by $v'/u' = -\epsilon\, \mathrm{d}A^*/\mathrm{d}x^*$.

The main part of the boundary layer (region 2 in figure 2) is the continuation of the upstream region β, and here the normal variable Y, defined in (2.3*a*), is related to $\hat{Y}$ in the intermediate layer by $Y = g_w^{n+1} \hat{Y}$. Substitution in the asymptotic forms (2.27) for large $\hat{Y}$ yields

$$u' = a Y^{\frac{1}{n+1}} + \ldots + g_w^{n+1/2} \chi^{1/4} a \frac{A^*(x^*)}{n+1} Y^{-\frac{n}{n+1}} + \ldots, \quad v' = -\epsilon a \frac{\mathrm{d}A^*}{\mathrm{d}x^*} Y^{\frac{1}{n+1}}, \tag{2.29a, b}$$

with an enthalpy expansion similar to that for u'. This suggests the following expansions:

$$(u', h') = \{\tilde{U}_0(Y), \tilde{H}_0(Y)\} + g_w^{n+1/2}\chi^{1/4}\{\tilde{U}_1(x^*, Y), \tilde{H}_1(x^*, Y)\} + \ldots, \quad (2.30a, b)$$

$$v' = \epsilon\tilde{V}_1(x^*, Y) + \ldots, \quad \rho' = M_\infty^{-2}\{\tilde{R}_0(Y) + g_w^{n+1/2}\chi^{1/4}\tilde{R}_1(x^*, Y) + \ldots\}, \quad (2.30c, d)$$

in region 2, with the pressure given by (2.19*e*). The solution in region 2 must match that in the upstream boundary layer (region β) as $x^* \to -\infty$ and therefore $\tilde{U}_0$, $\tilde{H}_0$ and $\tilde{R}_0$ may be regarded as known functions, describing the solution of (2.4) in the limit $x \to 1$ and satisfying conditions (2.8).

The solution for the perturbation functions $\tilde{U}_1$, $\tilde{V}_1$, $\tilde{R}_1$, and $\tilde{H}_1$ is given in Appendix A, and it follows that the slope of the streamlines at the outer edge of region 2 is

$$v'/u' \to \epsilon\left\{-\frac{\mathrm{d}A^*}{\mathrm{d}X^*} + S^*\mathscr{L}\frac{\mathrm{d}p^*}{\mathrm{d}x^*}\right\} \quad \text{as} \quad Y \to \delta_0, \quad (2.31)$$

where δ_0 is the thickness of the upstream boundary layer evaluated as $x \to 1$ and

$$\mathscr{L} = \int_0^{\delta_0}\left(\frac{1}{M_0^2} - 1\right)\mathrm{d}Y. \quad (2.32)$$

Here $M_0(Y)$ is the Mach number distribution across the boundary layer just upstream of the interaction region. The dimensionless parameter S^* is defined by

$$S^* = M_\infty^{1/2} g_w^{-(n+1/2)} Re_0^{-1/8} = \chi^{1/4} g_w^{-(n+1/2)}, \quad (2.33)$$

and it should be noted that if g_w is $O(1)$, $S^* \ll 1$. However, for a sufficiently cold wall ($g_w \ll 1$), S^* may be $O(1)$ or even $S^* \gg 1$. The first term on the right-hand side of (2.31) is the conventional displacement effect associated with the sublayer, while the second term is the contribution due to the main part of the boundary layer.

To complete the formulation of the interaction problem, an inviscid potential flow (region 3, figure 2) outside the boundary layer must be considered, and here the characteristic independent variables are x^* and Y^*, defined $y' = M_\infty^{-1}\chi^{3/4} g_w^{n+1/2} Y^*$. The scaling for the dependent variables can be determined from (2.31) and

$$(u', v', h') = (1, 0, h_\infty U_\infty^{-2}) + \epsilon(M_\infty^{-1}u_1, v_1, M_\infty^{-1}h_1) + \ldots, \quad (2.34a\text{–}c)$$

$$(p', \rho') = (1, 1) + \chi^{1/2}(\gamma p_1, \rho_1) + \ldots. \quad (2.34d, e)$$

The perturbation functions u_1, v_1, p_1, ρ_1 and h_1 in these expansions are functions of (x^*, Y^*) and must vanish as $(x^{*2} + Y^{*2}) \to \infty$. From (2.31), matching to the main part of the boundary layer (region 2) requires

$$v_1(x^*, 0) = -\frac{\mathrm{d}A^*}{\mathrm{d}x^*} + S^*\mathscr{L}\frac{\mathrm{d}p^*}{\mathrm{d}x^*}. \quad (2.35)$$

Substitution of (2.34) into the Navier–Stokes equations leads to a familiar problem associated with linearized supersonic flow, and the solution gives

$$p^*(x^*) = p_1(x^*, 0) = -\frac{\mathrm{d}A^*}{\mathrm{d}x^*} + S^*\mathscr{L}\frac{\mathrm{d}p^*}{\mathrm{d}x^*}, \quad (2.36)$$

which defines the pressure distribution in the interaction zone. This law, together with (2.20) constitute the complete interaction problem in a region whose streamwise extent is M_∞ times greater than the thickness of the upstream hypersonic boundary layer.

Note for $\mathscr{L} > 0$, a pressure rise ($dp^*/dx^* > 0$) leads to an increase of displacement thickness of region 2, just as for a subsonic mainstream flow. On the other hand, if $\mathscr{L} < 0$, a pressure rise produces a decrease in the displacement thickness as in supersonic flows. Consequently, a boundary layer with $\mathscr{L} > 0$ is referred to as subcritical and that with $\mathscr{L} < 0$ is called supercritical (Neiland 1973). For supersonic flows with large mainstream Mach number, the supercritical case is expected to be most common. For example, it can be shown that if viscosity depends linearly on temperature ($n = 1$), the Blasius solution is supercritical for $\gamma < 2.37$ and subcritical for $\gamma > 2.37$.

2.4. *The general interaction problem*

The interaction problem may be cast in a general form through scaling transformations and a Prandtl transposition according to

$$x^* = \lambda^{-1/2} c\bar{x}, \quad y^* = c(\bar{y} + \bar{Y}_0), \quad Y_0^* = c\bar{Y}_0, \quad A^* = c(\bar{A} - \bar{Y}_0), \tag{2.37a–d}$$

$$u^* = \lambda c\bar{u}, \quad v^* = c\lambda^{3/2}\left(\bar{v} + \bar{u}\frac{d\bar{Y}_0}{d\bar{x}}\right), \quad p^* = \lambda^{1/2}\bar{p}, \tag{2.37e–g}$$

where the constant $c = (\gamma - 1)^{1/2}\lambda^{-3/4}$; equations (2.20) and (2.36) become

$$\bar{u}\frac{\partial \bar{u}}{\partial \bar{x}} + \bar{v}\frac{\partial \bar{u}}{\partial \bar{y}} = -\frac{d\bar{p}}{d\bar{x}} + \frac{\partial^2 \bar{u}}{\partial \bar{y}^2}, \quad \frac{\partial \bar{u}}{\partial \bar{x}} + \frac{\partial \bar{v}}{\partial \bar{y}} = 0, \tag{2.38a, b}$$

$$\bar{p} = -\frac{d\bar{A}}{d\bar{x}} + \frac{d\bar{Y}_0}{d\bar{x}} + S\mathscr{L}\frac{d\bar{p}}{d\bar{x}}, \tag{2.38c}$$

where

$$S = (\gamma - 1)^{-1/2}\lambda^{5/4}S^*. \tag{2.39}$$

Solutions of this system depend on the level of wall cooling, characterized by the magnitude of S or equivalently the Neiland number defined by

$$N = (S|\mathscr{L}|)^{4/3}. \tag{2.40}$$

Three regimes are immediately evident corresponding to: (i) $N \ll 1$, for $g_w \gg \chi^{1/(4n+2)}$; (ii) $N = O(1)$, for $g_w \sim \chi^{1/(4n+2)}$; (iii) $N \gg 1$, for $g_w \ll \chi^{1/(4n+2)}$. In the first of these regimes $S \ll 1$ and the interaction problem (2.38) reduces to that considered by Jenson, Burggraf & Rizetta (1975) and Ruban (1978), wherein condition (2.38c) becomes a conventional Ackeret law. Numerical solutions in the second regime have been obtained by Brown *et al.* (1990) and Cassel (1993) and generally show that wall cooling acts to inhibit separation. The situations of interest in the present study correspond to the third regime with strong wall cooling in the sense that $N \to \infty$.

For N large, the following scaled variables are indicated:

$$x = N^{-3/4}\bar{x}, \quad y = N^{-1/4}\bar{y}, \quad u = N^{-1/4}\bar{u}, \quad v = N^{1/4}\bar{v}, \tag{2.41a–d}$$

$$p = N^{-1/2}\bar{p}, \quad A = N^{-1/4}\bar{A}, \quad \bar{Y}_0 = N^{5/4}F. \tag{2.41e–g}$$

Substitution in (2.38) yields

$$\frac{\partial \psi}{\partial y}\frac{\partial^2 \psi}{\partial x\,\partial y} - \frac{\partial \psi}{\partial x}\frac{\partial^2 \psi}{\partial y^2} = -\frac{dp}{dx} + \frac{\partial^3 \psi}{\partial y^3}, \quad u = \frac{\partial \psi}{\partial y}, \tag{2.42}$$

with the interaction law

$$p = \operatorname{sgn}(\mathscr{L})\frac{dp}{dx} + \frac{dF}{dx} - \frac{1}{N}\frac{dA}{dx}, \tag{2.43}$$

and the boundary conditions

$$\psi = \frac{\partial \psi}{\partial y} = 0 \quad \text{at} \quad y = 0, \quad \psi \to \tfrac{1}{2}y^2 \quad \text{as} \quad x \to -\infty \tag{2.44a–c}$$

$$\psi \to \tfrac{1}{2}y^2 + A(x)\,y + \ldots \quad \text{as} \quad y \to +\infty. \tag{2.45}$$

The interaction problem depends on two parameters. The Neiland number N represents the ratio of the contributions to the displacement thickness from the main part of the boundary layer (region 2) and the viscous sublayer (region 1). The second parameter is the scaled ramp angle defined by

$$\beta = \theta_0 \lambda^{-1/2} N^{-1/2}, \tag{2.46}$$

where the body contour is described by

$$F = 0 \quad \text{for} \quad x < 0; \quad F = \beta x \quad \text{for} \quad x > 0. \tag{2.47a, b}$$

The problem $N \to \infty$ has also been considered by Brown *et al.* (1990), and the relation of this work to the present study is described in Appendix B. It should be noted that an additional regime exists for very high levels of wall cooling. As $g_w \to 0$, the thickness of the upstream layer α in figure 2 shrinks at a faster rate than the sublayer 1, according to (2.9*c*), (2.19*b*) and (2.41*b*); it can easily be shown that both layers have comparable thickness when $g_w = O(\chi^{1/(n+2)})$. Consequently the interaction problem (2.42)–(2.45) is valid for large N in the range

$$\chi^{1/(n+2)} \ll g_w \ll \chi^{1/(4n+2)}, \tag{2.48}$$

or alternatively $1 \ll N \ll \chi^{-n/(n+2)}$. Therefore a fourth regime exists for $g_w = O(\chi^{1/(n+2)})$, wherein compressibility effects must be taken into account in the viscous sublayer 1, in view of the fact that matching to the upstream region α requires that the density and enthalpy are dependent on y.

3. Supercritical separation

3.1. *Introduction*

In the present study, a theory is constructed for large N, wherein the dominant contribution to displacement thickness is due to the main part of the boundary layer; this may be described as an inviscid–inviscid interaction between regions 2 and 3 (see figure 2). The form of the interaction law (2.43) suggests the following expansions, for scaled ramp angles β of $O(1)$:

$$p = p_0(x) + N^{-1}p_1(x) + \ldots, \quad A(x) = A_0(x) + N^{-1}A_1(x) + \ldots, \tag{3.1a, b}$$

and the leading-order term for pressure then satisfies

$$p_0 = \operatorname{sgn}(\mathscr{L})\frac{\mathrm{d}p_0}{\mathrm{d}x} + \beta H(x), \tag{3.2}$$

where H is the Heaviside function. For the supercritical case ($\mathscr{L} < 0$), the solution of (3.2) which is finite as $x \to -\infty$ (Neiland & Sokolov 1975)

$$p_0 = 0 \quad \text{if} \quad x < 0; \quad p_0 = \beta(1 - \mathrm{e}^{-x}) \quad \text{if} \quad x > 0. \tag{3.3}$$

Thus the flow is undisturbed upstream of the corner and the pressure starts to rise at $x = 0$, tending smoothly to β as $x \to \infty$.

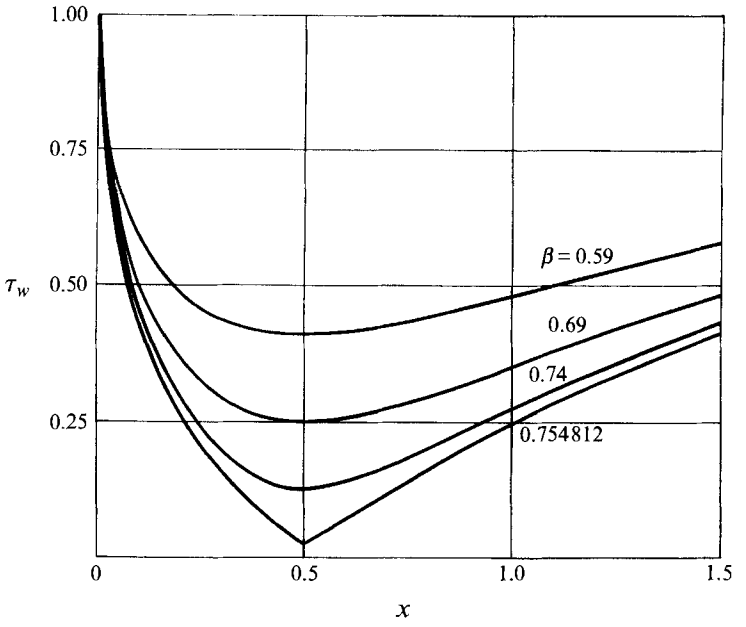

FIGURE 3. Variation of wall shear stress for increasing dimensionless ramp angle β.

In the sublayer (region 1), the stream function ψ may be written

$$\psi = \psi_0(x,y) + N^{-1}\psi_1(x,y) + \ldots, \tag{3.4}$$

and substitution of (3.1) and (3.4) into (2.42) gives

$$\frac{\partial\psi_0}{\partial y}\frac{\partial^2\psi_0}{\partial x\,\partial y} - \frac{\partial\psi_0}{\partial x}\frac{\partial^2\psi_0}{\partial y^2} = -\frac{\mathrm{d}p_0}{\mathrm{d}x} + \frac{\partial^3\psi_0}{\partial y^3}, \tag{3.5}$$

with boundary conditions

$$\psi_0 = \frac{\partial\psi_0}{\partial y} = 0 \quad \text{at} \quad y = 0; \quad \psi_0 \to \tfrac{1}{2}y^2 + A_0(x)y + \ldots \quad \text{as} \quad y \to +\infty, \tag{3.6}$$

and the initial condition

$$\psi_0 \to \tfrac{1}{2}y^2 \quad \text{as} \quad x \to -\infty. \tag{3.7}$$

Therefore the sublayer problem is a conventional boundary layer with pressure gradient prescribed by (3.3).

Since p_0 and hence A_0 are zero for $x < 0$, the initial condition (3.7) was used to initiate a step-by-step integration of (3.5) starting from $x = 0$. Calculations were carried out using a standard Crank–Nicolson method for a number of mesh sizes and the results are believed to be grid independent. Calculated results for skin friction distribution $\tau_w = \partial^2\psi_0/\partial y^2$ at $y = 0$ are shown in figure 3 for increasing values of the ramp angle β. It may be seen that $\tau_w(x)$ initially decreases and then subsequently reaches a minimum at a location downstream of the corner $x = 0$. The skin friction then recovers as $x \to \infty$ toward a value appropriate to a constant-pressure boundary layer far downstream of the corner. With increasing ramp angle β, the minimum in τ_w decreases and finally reaches zero at a critical value $\beta_0 = 0.7548$ at $x = x_0 = 0.50$. This phenomenon is known as marginal separation (Ruban 1981; Stewartson, Smith & Kaups 1982). The behaviour of τ_w near the point of zero skin friction is shown in

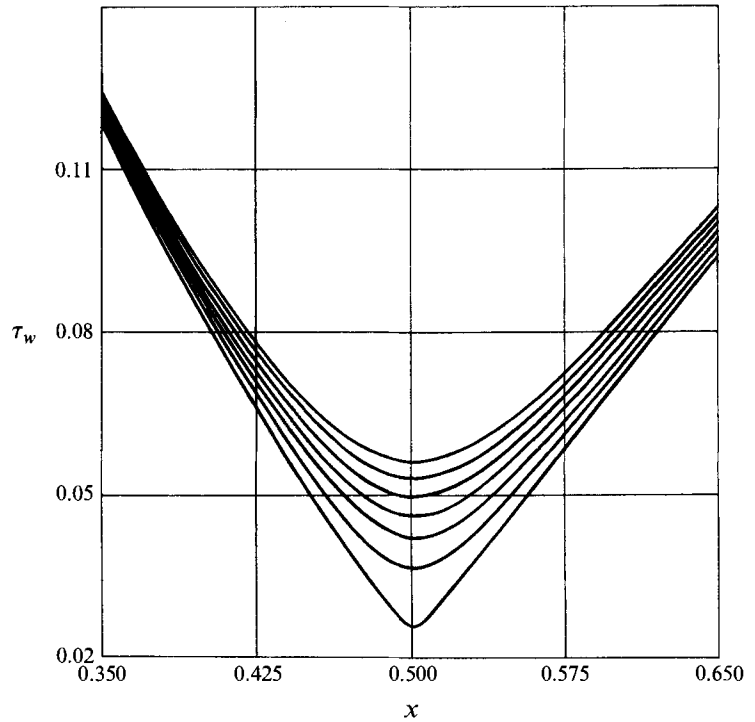

FIGURE 4. Wall-shear-stress distribution near the critical location $x_0 = 0.5$ and ramp angle β_0; lowest curve is $\beta = 0.7548$ and τ_w is plotted for increments $\Delta\beta = 0.0003$.

figure 4 for ramp angles approaching the critical value β_0 in steps of $\Delta\beta = 0.0003$. Note that τ_w is almost linear on either side of x_0 as $\beta \to \beta_0$.

Exactly the same behaviour occurs in the incompressible boundary layer near the leading edge of a thin airfoil at a critical angle of attack (Werle & Davis 1972). A detailed analysis (Ruban 1981) shows that, as the critical angle of attack is approached from below, a singularity develops at the point of zero skin friction. However, in contrast to the Goldstein singularity, the singularity is 'weak' in the sense that it does not preclude continuation of the boundary-layer solution downstream beyond x_0. However, a discontinuity develops in the slope of the streamlines near the boundary-layer edge; thus a local singular behaviour near $x = x_0$ is induced in the pressure field and an interaction region develops which has been analysed by Stewartson *et al.* (1982) and Ruban (1982). To distinguish this situation from self-induced separation, the phenomenon is referred to as marginal separation and is described by the solution of an integro-differential equation for the skin friction distribution along the airfoil contour in an interaction region centred on x_0, having a streamwise extent of $O(Re^{-1/5})$. Stewartson *et al.* (1982) and Ruban (1982) considered perturbations of $O(\bar{a}Re^{-2/5})$ about the critical angle of attack β_0 and obtained numerical solutions of the integro-differential equation for different values of the parameter $\bar{a}$. At a critical positive value of $\bar{a}$, say $\bar{a}_s$, the skin friction at a particular streamwise location vanishes, and for $\bar{a} > \bar{a}_s$, the appearance of a short separation bubble in the interaction region near the leading edge of the airfoil is predicted. However, there are no solutions of the problem for $\bar{a}$ larger than a second critical value $\bar{a}_b$, with $\bar{a}_b > \bar{a}_s$. In accordance with experiment, this suggests that for angles of attack beyond a critical value, the short bubble 'bursts', giving rise to an extended separation region on the upper surface of the airfoil. It was

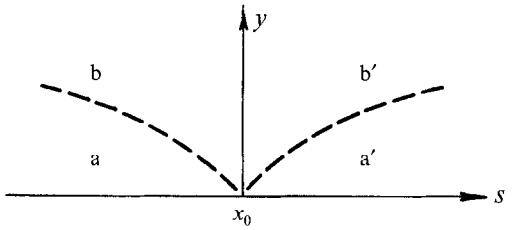

FIGURE 5. Schematic diagram of the sublayer structure near the marginal separation point.

also shown by Brown & Stewartson (1983) that in the range $\bar{a}_s < \bar{a} < \bar{a}_b$, there are at least two solutions, one of which corresponds to a relatively long separation region. This non-uniqueness suggests that a hysteresis effect and possible fluctuations in the airfoil lift and drag may occur near the critical angle of attack.

3.2. *Structure near marginal separation*

It will now be demonstrated that marginal separation theory applies to supercritical hypersonic separation on a cold wall. Let $\Psi_{00}(y)$ denote the stream function at $x = x_0$ for the critical ramp angle β_0; in principle, Ψ_{00} may be found through a numerical integration of (3.5) as $x \to x_0$ and is of the form

$$\Psi_{00} \to \tfrac{1}{6}\lambda_0 y^3 - \frac{2\lambda_0^2}{7!} y^7 + \frac{\lambda_0 a_0^2}{8!} y^9 + \ldots \quad \text{as} \quad y \to 0 \tag{3.8}$$

(Stewartson *et al.* 1982; Ruban 1981), where a_0 is a constant. Here λ_0 is the leading term in an expansion about x_0 for the pressure gradient, and from (3.3)

$$\frac{\mathrm{d}p_0}{\mathrm{d}x} = \lambda_0 - \lambda_0 s + \ldots \quad \text{as} \quad s \to 0, \tag{3.9}$$

where $s = x - x_0$ and $\lambda_0 = \beta_0 \mathrm{e}^{-x_0}$. Furthermore,

$$\Psi_{00} \to \tfrac{1}{2}y^2 + A_0(x_0)\, y + \ldots \quad \text{as} \quad y \to \infty, \tag{3.10}$$

where $A_0(x_0)$ may be regarded as a known constant.

Upstream of x_0, the sublayer (region 1) splits into two layers as shown schematically in figure 5 (Ruban 1981). In the near-wall viscous layer, denoted as region a, the solution of (3.5) is of the form

$$\psi_0 = \tfrac{1}{6}\lambda_0 \xi^3 \eta^3 + \tfrac{1}{2} a_0 \xi^6 \eta^2 + \xi^7 \left(\tfrac{1}{6}\lambda_0 \eta^3 - 2\lambda_0^2 \frac{\eta^7}{7!} \right) + \xi^9 f_2(\eta) + \ldots, \tag{3.11}$$

where

$$\xi = (-s)^{1/4}, \quad \eta = y/(-s)^{1/4}, \quad f_2(\eta) = \tfrac{1}{2} b_0 \eta^2 - \frac{a_0^2}{5!}\eta^5 + \frac{\lambda_0 a_0^2}{8!}\eta^9. \tag{3.12a–c}$$

The constants a_0 and b_0 may be found from a numerical solution of (3.5) and both a_0 and λ_0 are positive. Region b in figure 5 is a locally inviscid region where y is $O(1)$ and the solution matching (3.11) as $y \to 0$ is given by

$$\psi_0 = \Psi_{00}(y) + (-s)\, \Psi_{01}(y) + (-s)^{7/4}\, \Psi_{02}(y) + \ldots \quad \text{as} \quad s \to 0, \tag{3.13}$$

with

$$\Psi_{01} = \Psi'_{00} \left[\frac{a_0}{\lambda_0} + \int_0^y \frac{\lambda_0 - \Psi'''_{00}}{(\Psi'_{00})^2} \mathrm{d}y \right], \quad \Psi_{02} = \frac{b_0}{\lambda_0} \Psi'_{00}. \tag{3.14}$$

For marginal separation, the solution may be continued downstream of x_0 (Ruban 1981) and a similar analysis in regions a′, b′ of figure 5 shows that the expression

$$\psi_0 = \Psi_{00}(y) + \Psi'_{00}(y)\left[\frac{a_0}{\lambda_0}|s| + s\int_0^y \frac{\Psi'''_{00} - \lambda_0}{(\Psi'_{00})^2}\,\mathrm{d}y\right] + |s|^{7/4}\frac{b_0}{\lambda_0}\Psi'_{00}(y) + \ldots, \tag{3.15}$$

describes the stream function simultaneously in regions a, b, a′ and b′ of figure 5. Consequently, the wall shear stress

$$\tau_w = \left.\frac{\partial^2\psi_0}{\partial y^2}\right|_{y=0} \to a_0|s| + b_0|s|^{7/4} + \ldots \quad \text{as} \quad s \to 0, \tag{3.16}$$

in agreement with the numerical results shown in figure 4. In addition, it follows from (3.6), (3.10) and (3.15) that

$$A_0(x) = A_0(x_0) + \frac{a_0}{\lambda_0}|s| + I_0 s + \frac{b_0}{\lambda_0}|s|^{7/4} + \ldots \quad \text{as} \quad s \to 0, \tag{3.17}$$

where I_0 is a constant defined by

$$I_0 = \int_0^\infty \frac{\Psi'''_{00} - \lambda_0}{(\Psi'_{00})^2}\,\mathrm{d}y. \tag{3.18}$$

It is evident that the displacement function, as well as the streamlines in region 1, have a discontinuous slope at $x = x_0$.

The leading-order sublayer solution (3.15) alters the pressure distribution near x_0, and to evaluate the pressure perturbation $p_1(x)$ in (3.1*a*), the scaled ramp angle β is written in the form

$$\beta = \beta_0 + N^{-1}\beta_1 + \ldots, \tag{3.19}$$

to consider perturbations about the critical ramp angle β_0, where β_1 is an $O(1)$ variable. Substitution of (3.1) and (3.19) into the interaction law (2.43) yields

$$p_1 = -\frac{\mathrm{d}p_1}{\mathrm{d}x} + \beta_1 - \frac{\mathrm{d}A_0}{\mathrm{d}x}, \tag{3.20}$$

and the solution which vanishes as $x \to -\infty$ has $p_1(x) \equiv 0$ for $x < 0$ and

$$p_1(x) = \mathrm{e}^{-x}\int_0^x \mathrm{e}^t\left\{\beta_1 - \frac{\mathrm{d}A_0}{\mathrm{d}x}\right\}\mathrm{d}t \quad \text{for} \quad x > 0. \tag{3.21}$$

Thus $p_1(x)$ is continuous everywhere, but the pressure gradient $\mathrm{d}p_1/\mathrm{d}x$ has a jump discontinuity at $x = x_0$ described by

$$\frac{\mathrm{d}p_1}{\mathrm{d}x} = -p_1(x_0) + \beta_1 - I_0 + \begin{cases} a_0/\lambda_0 & \text{at} \quad s = 0^- \\ -a_0/\lambda_0 & \text{at} \quad s = 0^+. \end{cases} \tag{3.22}$$

The question now arises as to whether this jump provokes the formation of an additional inner interaction region near $x = x_0$, where the pressure distribution depends on the displacement thickness of both the viscous sublayer and the main part of the boundary layer (regions 1 and 2 in figure 2 respectively). Such an inner interaction region must be centred on x_0 and involve a shorter streamwise scale, which can be estimated using the marginal separation analysis of Ruban (1981).

Returning to the near-wall expansion (3.11) in region a, it may be readily inferred that the first and third terms arise from the pressure gradient. The second term contains

an eigenfunction $\frac{1}{2}a_0\eta^2$, and the exponent in the streamwise dependence $(-s)^{3/2}$ is determined from a detailed analysis (Ruban 1981) of the equation for $f_2(\eta)$, appearing in the fourth term of (3.11), in which all solutions having exponential growth as $\eta \to \infty$ must be ruled out. Now suppose that in a region near x_0, the second-order pressure gradient induced by the sublayer $N^{-1}\,\mathrm{d}p_1/\mathrm{d}x$ becomes large enough to be included in the equation for $f_2(\eta)$, thereby potentially altering the whole expansion (3.11). This defines the occurrence of the inner interaction region, and to estimate its streamwise extent, any term in the boundary-layer equation (3.5) associated with $f_2(\eta)$ may be used. In particular the viscous term is $(-s)^{3/2}f_2'''(\eta)$ and this becomes comparable to $N^{-1}\,\mathrm{d}p_1/\mathrm{d}x$ when

$$s = x - x_0 = O(N^{-2/3}), \tag{3.23}$$

since it is evident from (3.22) that $\mathrm{d}p_1/\mathrm{d}x$ is $O(1)$; this argument yields a preliminary estimate of the extent of the inner interaction region.

3.3. *Higher-order terms*

Substitution of (3.1) and (3.4) into (2.42) leads to the following linear problem for $\psi_1(x,y)$:

$$\frac{\partial\psi_0}{\partial y}\frac{\partial^2\psi_1}{\partial x\,\partial y}+\frac{\partial^2\psi_0}{\partial x\,\partial y}\frac{\partial\psi_1}{\partial y}-\frac{\partial\psi_0}{\partial x}\frac{\partial^2\psi_1}{\partial y^2}-\frac{\partial^2\psi_0}{\partial y^2}\frac{\partial\psi_1}{\partial x}=-\frac{\mathrm{d}p_1}{\mathrm{d}x}+\frac{\partial^3\psi_1}{\partial y^3}, \tag{3.24}$$

with

$$\psi_1=\frac{\partial\psi_1}{\partial y}=0 \quad \text{at} \quad y=0; \quad \psi_1\to A_1(x)\,y \quad \text{as} \quad y\to\infty, \tag{3.25}$$

and $\psi_1 \to 0$ as $x \to -\infty$. The solution of (3.24) in the near-wall layer a immediately upstream of x_0 consists of a discrete set of eigensolutions (Ruban 1981), each of which generates a series in powers of $\xi = (-s)^{1/4}$, having the form

$$\psi_1 = \{\xi^{-2}g_1(\eta)+\xi g_2(\eta)+O(\xi^4)\}+\{\xi^2 h_1(\eta)+O(\xi^5)\}+\tfrac{1}{6}\mu_0\,\xi^3\eta^2+\ldots, \tag{3.26}$$

where η is defined in (3.12*b*); the expansion (3.26) is based on the limit process $\xi \to 0$ with $\eta = O(1)$ and the constant μ_0 is defined by

$$\mu_0 = \lim_{x\to x_0^-}\frac{\mathrm{d}p_1}{\mathrm{d}x} = -p_1(x_0)+\beta_1-I_0+\frac{a_0}{\lambda_0}. \tag{3.27}$$

The eigenfunctions in (3.26) that do not exhibit exponential growth as $\eta \to \infty$ are (Ruban 1981)

$$g_1 = \tfrac{1}{2}a_1\eta^2, \quad g_2 = \tfrac{1}{2}b_1\eta^2, \quad h_1 = \tfrac{1}{2}c_1\eta^2, \tag{3.28}$$

where a_1, b_1 and c_1 are arbitrary constants; however, the equation for g_2 depends on g_1 and it can easily be shown that b_1 is proportional to a_1. According to (3.26)

$$\left.\frac{\partial^2\psi_1}{\partial y^2}\right|_{y=0} \to \frac{a_1}{(-s)}+\frac{b_1}{(-s)^{1/4}}+c_1+\ldots \quad \text{as} \quad s\to 0^-, \tag{3.29}$$

and hence a_1 and c_1 can, in principle, be estimated as functions of β_1 from a numerical solution of (3.24) initiated at $x = 0$.

In region b of figure 5, y is $O(1)$ and the solution of (3.24) matching (3.26) in region a is of the form

$$\psi_1 = \frac{1}{(-s)}\frac{a_1}{\lambda_0}\Psi_{00}'(y)+(-s)^{-1/4}\frac{b_1}{\lambda_0}\Psi_{00}'(y)+\Psi_{13}(y)+\ldots \quad \text{as} \quad s\to 0^-. \tag{3.30}$$

The function Ψ_{13} satisfies the matching condition

$$\Psi_{13}(y) \to \tfrac{1}{2}c_1 y^2 + \tfrac{1}{6}\mu_0 y^3 \ldots \quad \text{as} \quad y \to 0, \tag{3.31}$$

and a complicated equation involving Ψ_{00} which is omitted here. Using (3.10), (3.25) and (3.30), the behaviour of ψ_1 as $y \to \infty$ may be determined and hence A_1 is found to be of the form

$$A_1 = \frac{1}{(-s)}\frac{a_1}{\lambda_0} + \frac{1}{(-s)^{1/4}}\frac{b_1}{\lambda_0} + \ldots \quad \text{as} \quad s \to 0^-. \tag{3.32}$$

The solution (3.4), comprising (3.11) and (3.26) in region a and (3.15) and (3.30) in region b, is not uniformly valid near $x = x_0$. As a result of the unbounded growth of $(-s)^{-1/2}g_1(\eta)$, the first eigenfunction in (3.26) becomes comparable with the second term in (3.11) when $(-s) \sim N^{-1/2}$; a similar conclusion is reached by comparing the first term in (3.30) with the second term in (3.13). It therefore appears that expansion (3.4) becomes disordered when

$$s = (x - x_0) = O(N^{-1/2}). \tag{3.33}$$

This suggests a much larger interaction region than the previous estimate (3.23) within which the perturbation pressure p_1 does not influence the sublayer solution to leading order. However, the estimate (3.33) is implicitly based on the assumption that a_1 is $O(1)$; it is now shown that a_1 must be $o(1)$ as $N \to \infty$ and that the original estimate (3.23) is correct.

In a marginal separation analysis near the leading edge of an airfoil at angle of attack, Ruban (1981) has considered a similar problem. When applied to the present problem, Ruban's (1981) analysis shows that the expansion (3.4), when continued into an inner interaction zone where $s = O(N^{-1/2})$, yields the following solution:

$$\psi_0 = \Psi_{00}(y) + \Psi'_{00}(y)\left[\frac{a_0}{\lambda_0}\left(s^2 + 2\frac{a_1}{a_0}N^{-1}\right)^{1/2} + s\int_0^y \frac{\Psi'''_{00} - \lambda_0}{(\Psi'_{00})^2}\,\mathrm{d}y\right]. \tag{3.34}$$

Evidently, a numerical solution of the boundary-value problem (3.24) will yield a different value of a_1 as $s \to 0^-$ for each value of β_1. For a_1 positive, the skin friction in the proposed inner interaction zone

$$\tau_w = \left.\frac{\partial^2 \psi}{\partial y^2}\right|_{y=0} = a_0\left(s^2 + 2\frac{a_1}{a_0}N^{-1}\right)^{1/2} \tag{3.35}$$

is positive everywhere, achieving a positive minimum at $s = 0$; the displacement function

$$A(x) = A(x_0) + I_0 s + \frac{a_0}{\lambda_0}\left(s^2 + 2\frac{a_1}{a_0}N^{-1}\right)^{1/2} \tag{3.36}$$

is smooth and therefore an inner interaction region does not form near $x = x_0$. On the other hand, for $a_1 < 0$, (3.34) exists only upstream of the point of zero skin friction which occurs at

$$x_s = x_0 - \left(2\frac{|a_1|}{a_0}N^{-1}\right)^{1/2}, \tag{3.37}$$

and where a Goldstein singularity develops. The interpretation of these results is as follows. Starting with large negative values of β_1, integration of (3.24) yields positive values of a_1 and a point of zero skin friction does not occur. However, for some critical $O(1)$ value, say $\beta_1 = \beta_{1c}$, $a_1 = 0$ and the ramp angle β cannot be increased since larger values of β_1 provoke a Goldstein singularity. The solution structure close to this critical angle is now considered.

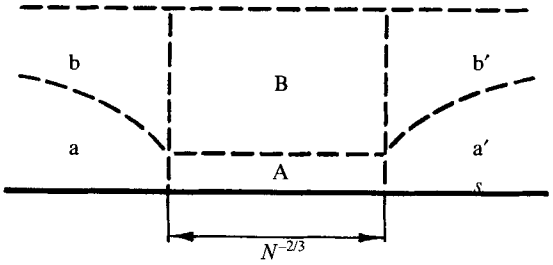

FIGURE 6. Sketch of the structure of the inner interaction region (not to scale).

Since the lengthscale (3.33) is not relevant when a_1 is small, consider again the estimate (3.23), and it follows that the contribution of the first term in (3.32) to the displacement function is comparable to the term $O(s)$ in (3.17) if $a_1 \sim N^{-1/3}$. This suggests the following continuations of expansions (3.1) and (3.4):

$$(A, p, \psi) = (A_0, p_0, \psi_0) + N^{-1}(A_1, p_1, \psi_1) + N^{-4/3}(A_2, p_2, \psi_2) + \dots. \tag{3.38}$$

The interaction law (3.2) suggests that the ramp angle should be written

$$\beta = \beta_0 + N^{-1}\beta_{1c} + N^{-4/3}\tilde{\beta}, \tag{3.39}$$

and it is easily shown that $p_2(x) = \tilde{\beta}(1-\mathrm{e}^{-x})$; here $\tilde{\beta}$ is a parameter which may be either positive or negative. The problem for ψ_2 is the same as (3.24) and, consequently, the solution for ψ_2 in regions a and b is essentially the same as in (3.26) and (3.30) respectively. Denoting $\tilde{a}_1$ and $\tilde{b}_1$ as the analogue of the coefficients of the eigenfunctions in (3.30), it is evident that different values of $\tilde{\beta}$ will give rise to values of $\tilde{a}_1$ which can be obtained from a numerical solution for ψ_2. Since the problem for ψ_2 is linear, $\tilde{a}_1$ may be regarded as proportional to $\tilde{\beta}$. Moreover (3.26) and (3.30) may still be considered to apply *but with* a_1 *replaced by* $a_1 = N^{-1/3}\tilde{a}_1$.

3.4. *The inner interaction region*

In this region, a new longitudinal variable is defined from (3.23),

$$s = x - x_0 = N^{-2/3}X_*, \tag{3.40}$$

and it may be inferred from (3.17), (3.22) and (3.32) that $A(x)$ and the pressure $p(x)$ should be expanded as

$$A = A_0(x_0) + N^{-2/3}A_*(X_*) + \dots, \tag{3.41}$$

$$p = p_0(x_0) + N^{-2/3}\lambda_0 X_* + N^{-1}p_1(x_0) + N^{-4/3}\tfrac{1}{2}\lambda_1 X_*^2 + N^{-5/3}P_*(X_*) + \dots, \tag{3.42}$$

where

$$A_* \to I_0 X_* + \frac{a_0}{\lambda_0}(-X_*) + \frac{\tilde{a}_1}{\lambda_0}(-X_*)^{-1} + \dots, \quad P_* \to \mu_0 X_* + \dots \quad \text{as} \quad X_* \to -\infty, \tag{3.43a, b}$$

with μ_0 defined by (3.27). Substitution into (2.43) then yields the inner interaction law

$$\frac{\mathrm{d}P_*}{\mathrm{d}X_*} = \beta_{1c} - p_1(x_0) - \frac{\mathrm{d}A_*}{\mathrm{d}X_*}. \tag{3.44}$$

The boundary-layer structure associated with the inner interaction region is shown schematically in figure 6. Region B is the continuation of inviscid layer b, and here it follows from (3.15) and (3.30) that ψ should be expanded as

$$\psi = \Psi_{00}(y) + N^{-2/3}\tilde{\Psi}_1(X_*, y) + N^{-1}\Psi_{13}(y) + N^{-7/6}\tilde{\Psi}_2(X_*, y) + \dots. \tag{3.45}$$

Substitution of (3.42) and (3.45) into the boundary-layer equations (2.42) leads to equations for $\tilde{\Psi}_1$ and $\tilde{\Psi}_2$ which have the solutions

$$\tilde{\Psi}_1(X_*, y) = \left[\frac{1}{\lambda_0} B_*(X_*) + X_* \int_0^y \frac{\Psi_{00}''' - \lambda_0}{(\Psi_{00}')^2} \mathrm{d}y\right] \Psi_{00}'(y), \tag{3.46a}$$

$$\tilde{\Psi}_2(X_*, y) = \frac{1}{\lambda_0} C_*(X_*)\, \Psi_{00}'(y). \tag{3.46b}$$

Here B_* and C_* are arbitrary functions which from (3.15) and (3.30) satisfy

$$B_*(X_*) \to a_0(-X_*) + \tilde{a}_1(-X_*)^{-1} + \ldots, \tag{3.47a}$$

$$C_*(X_*) \to b_0(-X_*)^{-7/4} + \ldots \quad \text{as} \quad X_* \to -\infty \tag{3.47b}$$

in order to match the solution in region b; in addition, from (2.45), (3.10), (3.18), (3.41) and (3.45), the function B_* is related to the displacement function A_* by

$$A_*(X_*) = \frac{1}{\lambda_0} B_*(X_*) + I_0 X_*. \tag{3.48}$$

The near-wall region A in figure 6 is the continuation of viscous layer a into the inner interaction region. The thickness of layer a decreases as $(-s)^{1/4}$ for small s and since s is $O(N^{-2/3})$ in the inner interaction region, it follows that the thickness of region A is $O(N^{-1/6})$. Consequently, the appropriate variables in this zone are X_* and $Y_* = N^{1/6} y$. It may be inferred from the solution in region a, described by (3.11) and (3.26), that the stream function in region A is of the form

$$\psi = \tfrac{1}{6}\lambda_0 N^{-1/2} Y_*^3 + N^{-1} \Psi_1^*(X_*, Y_*) + N^{-7/6}\left(-\frac{2\lambda_0^2}{7!} Y_*^7 - \tfrac{1}{6}\lambda_0 X_* Y_*^3\right)$$

$$+ N^{-4/3} \frac{c_1}{2} Y_*^2 + N^{-3/2} \Psi_2^*(X_*, Y_*) + \ldots. \tag{3.49}$$

The equations for Ψ_1^* and Ψ_2^* are obtained by substituting (3.49) into (2.42). It is easily verified that the solution for Ψ_1^* matching that in regions a and B is

$$\Psi_1^* = \tfrac{1}{2} B_*(X_*)\, Y_*^2, \tag{3.50}$$

with $B_*(X_*)$ still arbitrary, apart from the matching condition (3.47*a*). The function $B_*(X_*)$ is determined through consideration of the problem for Ψ_2^*, which is

$$\tfrac{1}{2}\lambda_0 Y_*^2 \frac{\partial^2 \Psi_2^*}{\partial X_* \partial Y_*} - \lambda_0 Y_* \frac{\partial \Psi_2^*}{\partial X_*} = \frac{\partial^3 \Psi_2^*}{\partial Y_*^3} - \frac{\mathrm{d}P_*}{\mathrm{d}X_*} - \tfrac{1}{2} B_* B_*' Y_*^2, \tag{3.51}$$

with

$$\Psi_2^* = \frac{\partial \Psi_2^*}{\partial Y_*} = 0 \quad \text{at} \quad Y_* = 0. \tag{3.52}$$

To match the solution (3.4), (3.11) and (3.26) in region a and the solution (3.45) and (3.46) in region B as $y \to 0$

$$\Psi_2^* \to \frac{\lambda_0 a_0^2}{8!} Y_*^9 + \frac{a_0^2}{5!} X_* Y_*^5 + \frac{1}{6}\mu_0 Y_*^3 + \tfrac{1}{2} C_*(X_*)\, Y_*^2 + \ldots$$

$$\text{as} \quad X_* \to -\infty \quad \text{and} \quad Y_* \to \infty, \tag{3.53}$$

respectively, while the interaction law (3.44) in terms of B_* is

$$\frac{\mathrm{d}P_*}{\mathrm{d}X_*} = \beta_{1c} - p_1(x_0) - I_0 - \frac{1}{\lambda_0}\frac{\mathrm{d}B_*}{\mathrm{d}X_*}. \tag{3.54}$$

The system of equations (3.51)–(3.54) constitutes the inner interaction problem and may be written in a more convenient form by defining new dependent variables

$$\Psi_2^* = \Psi_2 + \frac{\lambda_0 a_0^2}{8!} Y_*^9 + \frac{a_0^2}{5!} X_* Y_*^5 + \tfrac{1}{6}\mu_0 Y_*^3 + \frac{B_*^2 - a_0^2 X_*^2 - 2a_0\tilde{a}_1}{2\lambda_0} Y_*, \tag{3.55}$$

$$P_* = \mu_0 X_* + P_2, \tag{3.56}$$

and introducing the following affine transformations:

$$\Psi_2 = a_0^{1/2}\lambda_0^{-2}\Psi, \quad X_* = a_0^{-2/3}\lambda_0^{-1/3}X, \quad Y_* = a_0^{-1/6}\lambda_0^{-1/3}Y, \tag{3.57a–c}$$

$$P_2 = a_0^{1/3}\lambda_0^{-4/3}P, \quad B_* = a_0^{1/3}\lambda_0^{-1/3}B, \quad C_* = a_0^{5/6}\lambda_0^{-4/3}C. \tag{3.57d–f}$$

The inner interaction problem is now defined by

$$\tfrac{1}{2}Y^2\frac{\partial^2\Psi}{\partial X\partial Y} - Y\frac{\partial\Psi}{\partial X} = \frac{\partial^3\Psi}{\partial Y^3} - \frac{\mathrm{d}P}{\mathrm{d}X}, \quad \frac{\mathrm{d}P}{\mathrm{d}X} = -\frac{\mathrm{d}B}{\mathrm{d}X} - 1, \tag{3.58a, b}$$

with the boundary conditions

$$\Psi = 0, \quad \frac{\partial\Psi}{\partial Y} = -\tfrac{1}{2}(B^2 - X^2 + 2\tilde{a}) \quad \text{at} \quad Y = 0, \tag{3.59a, b}$$

$$\Psi \to \tfrac{1}{2}CY^2 - \tfrac{1}{2}(B^2 - X^2 + 2\tilde{a})\,Y\ldots \quad \text{as} \quad Y\to\infty, \quad \text{or as} \quad X\to-\infty. \tag{3.60}$$

Here $\tilde{a}$ is a similarity parameter defined by $\tilde{a} = -\tilde{a}_1 a_0^{1/3}\lambda_0^{2/3}$, which is proportional to $\tilde{\beta}$, since $\tilde{a}_1$ is proportional to $\tilde{\beta}$. Recall that $N^{-4/3}\tilde{\beta}$ is the deviation of the ramp angle β from its critical value $\beta_0 + N^{-1}\beta_{1c}$. Lastly, the matching conditions (3.47) to the solution upstream in region b become

$$B(X) \to -X + \tilde{a}/X + \ldots, \quad C(X) \to \tilde{b}(-X)^{7/4} + \ldots \quad \text{as} \quad X\to-\infty, \tag{3.61}$$

where $\tilde{b} = b_0 a_0^2 \lambda_0^{-3/4}$. Downstream of the interaction region, matching to region b′ requires that

$$B(X) \to X + \ldots \quad \text{as} \quad X\to\infty. \tag{3.62}$$

It was shown by Stewartson (1970) and Ruban (1982) that the solution for (3.58) exists and is not exponentially large at $Y\to\infty$, only if the right-hand side of the boundary condition (3.59*b*) and the pressure gradient satisfy the following compatibility condition:

$$\tfrac{1}{2}(B^2 - X^2 + 2\tilde{a}) = -\frac{\bar{\lambda}}{2}\int_{-\infty}^{X}\frac{P'(\xi)}{(X-\xi)^{1/2}}\mathrm{d}\xi, \quad \bar{\lambda} = \frac{\Gamma(\frac{3}{4})}{\sqrt{2}\,\Gamma(\frac{5}{4})}, \tag{3.63}$$

where Γ denotes Gamma function. This is the fundamental equation of marginal separation theory. In the present case, the interaction law (3.58*b*) gives the governing integro-differential equation for $B(X)$:

$$B^2 - X^2 + 2\tilde{a} = \bar{\lambda}\int_{-\infty}^{X}\frac{B'(\xi)+1}{(X-\xi)^{1/2}}\mathrm{d}\xi. \tag{3.64}$$

It may be noted that because the interaction law (3.58*b*) differs from that associated with the airfoil problem at angle of attack, the integrand in (3.64) is different from that in the problem considered by Ruban (1982) and Stewartson *et al.* (1982).

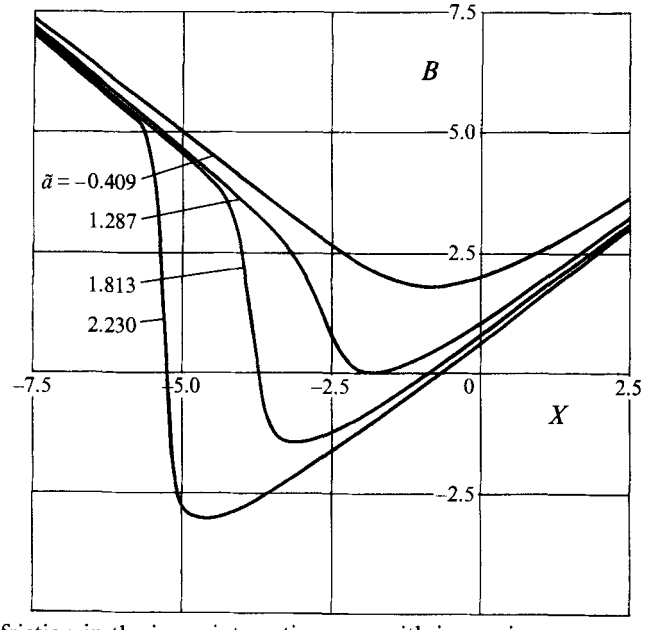

FIGURE 7. Skin friction in the inner interactive zone with increasing ramp angle (increasing $\bar{a}$).

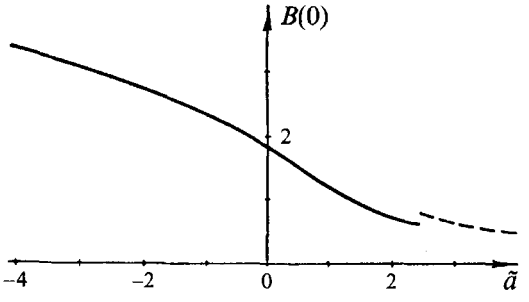

FIGURE 8. Dependence of $B(0)$ on the similarity parameter $\bar{a}$. Dashed line shows asymptotic result as $B(0) \to 2\bar{\lambda}^2/\bar{a} + \ldots$.

To obtain numerical solutions of (3.64), it is useful to develop expansions for B for large $|X|$, and using (3.61), (3.62) and (3.64) it may be shown that

$$B^2 - X^2 + 2\bar{a} \to -\tfrac{1}{2}\pi\bar{a}\bar{\lambda}(-X)^{-3/2} + \ldots \quad \text{as} \quad X \to -\infty, \tag{3.65a}$$

$$B^2 - X^2 + 2\bar{a} \to 4\bar{\lambda}X^{1/2} + \ldots \quad \text{as} \quad X \to \infty. \tag{3.65b}$$

Numerical solutions were obtained using the trapezoidal rule to approximate the right-hand side of (3.64) and the resulting set of nonlinear algebraic equations were solved using Newton iteration. It follows from (3.50) and (3.57*e*) that $B(X)$ is proportional to the skin friction, and distributions for various values of $\bar{a}$ are shown in figure 7. For values of $\bar{a}$ less than a critical value of 1.287, the skin friction is everywhere positive. On the other hand, for $\bar{a} > 1.287$, the negative values of B indicate the presence of a separation bubble in the boundary layer. As the ramp angle is increased (by increasing $\bar{a}$), the separation point moves progressively upstream; however, since the inner interaction region is centred on $x = x_0 = 0.5$ on the ramp, the separated region is always located downstream of the junction point of the ramp.

The dependence of $B(0)$ on the parameter $\bar{a}$ is shown in figure 8; $B(0)$ is unique and exists for all $\bar{a}$, in contrast to marginal separation at the leading edge of an airfoil

(Brown & Stewartson 1983), where the solution of the governing integro-differential equation exhibits non-uniqueness and does not exist above a certain value of $\tilde{a}$. It may be inferred from figure 7 that as $\tilde{a}$ increases, corresponding to increasing ramp angle, the solution for B develops a steep variation near the separation point X_s, which itself is large and negative. On the other hand the reattachment point X_r appears to approach zero. As X increases from left to right across X_s, B' changes abruptly from -1 to $+1$ through a layer of thickness $O(\tilde{a}^{-4})$; the solution as $\tilde{a}\to\infty$ may be constructed in a manner described by Brown & Stewartson (1983), and it can be shown that

$$X_s\to-\frac{\tilde{a}^2}{4\bar{\lambda}^2}-\frac{\bar{\lambda}^2}{\tilde{a}^2}+\ldots,\quad X_r\to-\frac{2\bar{\lambda}^2}{\tilde{a}}+\ldots\quad\text{as}\quad\tilde{a}\to\infty. \tag{3.66}$$

In addition, $B(0)\to 2\bar{\lambda}^2/\tilde{a}+\ldots$; this asymptotic result is shown as a dashed line in figure 8 and is in good agreement with the numerial calculation. In view of the behaviour of X_s indicated in (3.66), the present marginal separation theory merges into self-induced separation as the ramp angle is progressively increased with $\tilde{a}\to\infty$.

4. Subcritical separation

When the boundary layer approaching the corner (figure 1) is subcritical, $\mathscr{L}>0$ and for large values of N the leading term $p_0(x)$ in the pressure expansion (3.1) may be evaluated from the interaction law (2.43) (Neiland & Sokolov 1975) and

$$p_0=\beta\,\mathrm{e}^x\quad\text{for}\quad x<0;\quad p_0=\beta\quad\text{for}\quad x>0. \tag{4.1}$$

Since the pressure rises upstream of the corner and then is constant along the ramp, separation for $\mathscr{L}>0$ can only occur on the flat surface upstream of the corner (figure 1). Defining $x_0=\log\beta$, the pressure on the flat surface is $\exp(x+x_0)$; thus an increase in β leads to a parallel shift along the x-axis in the pressure distribution, which therefore has a universal form for all ramp angles. Because the boundary-layer problem (2.42)–(2.45) is invariant to the transformation $x\to x+x_0$, the leading-order pressure distribution (4.1) may be represented as $p_0(x)=\mathrm{e}^x$, which holds upstream of the ramp and the separation point. In contrast to the supercritical pressure distribution (3.3), there is no parameter that can be varied to alter the basic character of the boundary-layer flow; once the ramp angle β is sufficiently high, a point of zero skin friction will occur at a location denoted by $x=x_s$ and the appearance of a Goldstein (1948) singularity at x_s is inevitable.

The structure of the Goldstein singularity is well known. Unlike marginal separation (cf. (3.8)), the streamwise velocity profile at $x=x_s$ contains a term $O(y^4)$ for small y. As $s=x-x_s\to 0^-$, the viscous sublayer 1 (shown in figure 2) splits into a viscous near-wall layer denoted as region $\bar{\mathrm{a}}$ in figure 9, where y is $O((-s)^{1/4})$, and a locally inviscid layer denoted as $\bar{\mathrm{b}}$, where y is $O(1)$. The solution in the near-wall layer $\bar{\mathrm{a}}$ has the form

$$\psi_0=\tfrac{1}{6}\lambda_0\xi^3\eta^3+\xi^4 f_1(\eta)+\xi^5 f_2(\eta)+\ldots, \tag{4.2}$$

where ξ and η are as defined in (3.12a, b) and

$$f_1=\tfrac{1}{2}a_0\eta^2,\quad f_2=\tfrac{1}{2}b_0\eta^2-\frac{a_0^2}{240}\eta^5, \tag{4.3}$$

with η being finite at $s\to 0^-$. Here $\lambda_0=\mathrm{e}^{x_s}$ is the pressure gradient $\mathrm{d}p_0/\mathrm{d}x$ evaluated at $x=x_s$. The constants a_0 and b_0 are arbitrary but can, in principle, be obtained from a numerical solution of the system (3.5)–(3.7) with $p_0=\mathrm{e}^x$.

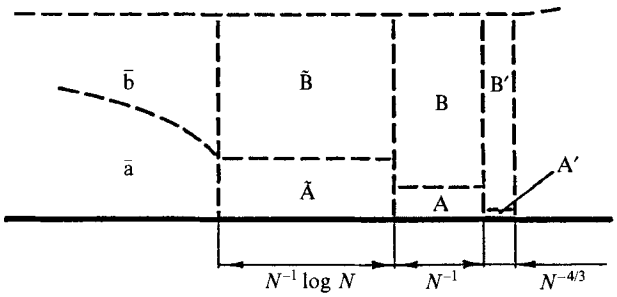

FIGURE 9. Schematic diagram of asymptotic structure in the sublayer near separation (not to scale).

In the inviscid region b̄

$$\psi_0 = \Psi_{00}(y)+(-s)^{1/2}\frac{a_0}{\lambda_0}\Psi'_{00}(y)+(-s)^{3/4}\frac{b_0}{\lambda_0}\Psi'_{00}(y)\ldots \quad \text{as} \quad s\to 0^-, \tag{4.4}$$

where the stream function at separation has

$$\Psi_{00} = \tfrac{1}{6}\lambda_0 y^3 - \frac{a_0^2}{240}y^5+\ldots \quad \text{as} \quad y\to 0, \tag{4.5}$$

to match with (4.2). At the external edge of layer b̄

$$\Psi_{00}\to \tfrac{1}{2}y^2 + A_0(x_s)y+\ldots \quad \text{as} \quad y\to\infty, \tag{4.6}$$

where $A_0(x_s)$ can be found from a global numerical solution. From (3.6) and (4.4) the displacement function upstream of separation has the form

$$A_0(x) = A_0(x_s)+\frac{a_0}{\lambda_0}(-s)^{1/2}+\frac{b_0}{\lambda_0}(-s)^{3/4}\ldots \quad \text{as} \quad s\to 0^-. \tag{4.7}$$

From (2.43), the next term in expansion (3.1*a*) satisfies

$$p_1 = \frac{\mathrm{d}p_1}{\mathrm{d}x} - \frac{\mathrm{d}A_0}{\mathrm{d}x}, \tag{4.8}$$

where $p_1\to 0$ as $x\to-\infty$. Clearly, $p_1(x)$ remains finite in the vicinity of x_s, but from (4.7) the pressure gradient is singular with

$$\frac{\mathrm{d}p_1}{\mathrm{d}x}\to -\frac{a_0}{2\lambda_0}(-s)^{-1/2}-\frac{3}{4}\frac{b_0}{\lambda_0}(-s)^{-1/4}+\ldots \quad \text{as} \quad s\to 0^-. \tag{4.9}$$

Using the same expansion (3.4) for ψ, the perturbation ψ_1 satisfies (3.24) and (3.25) with the pressure gradient given by (4.9). The boundary-value problem for ψ_1 is identical to that considered by Smith & Daniels (1981) in their study of the incompressible boundary-layer structure near a small hump on a wall. If the hump is located near $x=0$ with representation $y = hd^{1/3}Re^{-5/8}F(Re^{3/8}d^{-1}x)$, it is contained within the sublayer of a triple-deck structure. For the height parameter $h = O(1)$, solutions exhibiting reversed flow which are regular at separation are possible. Smith & Daniels (1981) considered the case of large h and small d and showed that the

boundary layer on the obstacle develops a Goldstein singularity on the downstream side of the hump. However, the singularity can be removed through consideration of a series of regions having successively shorter streamwise lengthscales, thereby permitting a smooth transition into a separated region downstream of the hump. In physical terms, this may be described as a 'compensation regime', in which the displacement thickness variation is identical to that of the shape of the obstacle but having the opposite sign; thus the combination of the hump shape and displacement cancel, leaving the slope of the streamlines at the outer edge of the boundary layer unaffected. This 'compensation' regime occurs when the hump extent is much smaller than the characteristic streamwise length of the interaction region (Smith *et al.* 1981). This is precisely the case here where the small vicinity of a point of zero skin friction is embedded deep within an interaction zone. Consequently, the analysis will follow the work of Smith & Daniels (1981), with a minimum of detail, in notation appropriate to the present problem.

The solution of (3.24) in the near-wall viscous layer $\bar{a}$ is of the form

$$\psi_1 = \log \xi \tilde{g}_1(\eta) + g_1(\eta) + \xi \log \xi \tilde{g}_2(\eta) + \xi g_2(\eta) + \ldots, \tag{4.10}$$

as $\xi \to 0$, with η being $O(1)$. The fourth term is forced by the singular pressure gradient (4.9), while the second term is necessary to prevent exponential growth for large η in $g_2(\eta)$. However, it emerges that $g_1(\eta)$ is itself an eigenfunction, and an additional term $\log \xi \tilde{g}_1(\eta)$ is required to avoid exponentially large behaviour in g_2 as $\eta \to \infty$. The solutions for $\tilde{g}_1$, g_1 and $\tilde{g}_2$ which are not exponentially large as $\eta \to \infty$ are

$$\tilde{g}_1(\eta) = \tfrac{1}{2}\tilde{a}_1 \eta^2, \quad g_1(\eta) = \tfrac{1}{2} a_1 \eta^2, \quad \tilde{g}_2(\eta) = \tfrac{1}{2}\tilde{a}_2 \eta^2, \tag{4.11}$$

and the equation for $g_2(\eta)$ is

$$g_2''' - \tfrac{1}{8}\lambda_0 \eta^3 g_2'' + \tfrac{1}{4}\lambda_0 \eta^2 g_2' - \tfrac{1}{4}\lambda_0 \eta g_2 = -\frac{a_0}{2\lambda_0} - \frac{a_0 \tilde{a}_1}{8}\eta^2. \tag{4.12}$$

The solution of this equation satisfying $g_2(0) = g_2'(0) = 0$ has been obtained by Smith & Daniels (1981) and is not exponentially large as $\eta \to \infty$ only if

$$\tilde{a}_1 = -(2\lambda_0)^{-1/2} \frac{\Gamma(\frac{3}{4})}{\Gamma(\frac{5}{4})}. \tag{4.13}$$

This determines the first eigenfunction in (4.11), and it may be shown that

$$g_2 = \tfrac{1}{2} a_2 \eta^2 - \frac{a_0 \tilde{a}_1}{\lambda_0} \eta \log \eta + \ldots \quad \text{as} \quad \eta \to \infty. \tag{4.14}$$

The constant a_2, as well as a_1 and $\tilde{a}_2$ which are associated with the other eigenfunctions in (4.11), are arbitrary but, in principle, could be found from a 'global' numerical solution of (3.24).

In region $\bar{b}$, the solution of (3.24) which matches with (4.10) as $y \to 0$ is of the form

$$\begin{aligned} \psi_1 = {} & (-s)^{-1/2} \log(-s) \frac{\tilde{a}_1}{4\lambda_0} \Psi_{00}'(y) + (-s)^{-1/2} \frac{a_1}{\lambda_0} \Psi_{00}'(y) \\ & + (-s)^{-1/4} \log(-s) \frac{\tilde{a}_2}{4\lambda_0} \Psi_{00}'(y) + (-s)^{-1/4} \frac{a_2}{\lambda_0} \Psi_{00}'(y) + \ldots. \end{aligned} \tag{4.15}$$

Because the leading terms in (4.10) and (4.15) are large as $s \to 0^-$, the expansion (3.4) is not uniformly valid. By comparing N^{-1} times the first term in (4.15) with the second

term in (4.4), it may be seen that a balance is achieved when $-s = O(N^{-1}\log N)$. Formally defining a new streamwise variable $\tilde{X}$ by

$$x = x_s + N^{-1}\log N\tilde{X}, \tag{4.16}$$

it may be inferred (as shown in figure 9) that two regions $\tilde{\mathrm{A}}$ and $\tilde{\mathrm{B}}$ occur near x_s, which are the continuations of zones $\bar{\mathrm{a}}$ and $\bar{\mathrm{b}}$, respectively. The form of ψ in the inviscid layer $\tilde{\mathrm{B}}$ may be inferred from (4.4), (4.15) and (4.16) and

$$\psi = \Psi_{00}(y) + \tilde{\epsilon}(\log N)\tilde{\psi}_1 + \tilde{\epsilon}(\log\log N)\tilde{\psi}_2 + \tilde{\epsilon}\tilde{\psi}_3 + \tilde{\epsilon}^{1/2}N^{-1/2}(\log N)\tilde{\psi}_4 + \tilde{\epsilon}^{1/2}N^{-1/2}(\log\log N)\tilde{\psi}_5 + \tilde{\epsilon}^{1/2}N^{-1/2}\tilde{\psi}_6 + \ldots, \tag{4.17}$$

where $\tilde{\epsilon} = N^{-1/2}\log^{-1/2}N$, and $\tilde{\epsilon}\to 0$ as $N\to\infty$. Here, $\tilde{\psi}_i = \tilde{\psi}_i(\tilde{X}, y)$ and substitution of (4.17) into (2.42) leads to

$$\Psi'_{00}(y)\frac{\partial^2\tilde{\psi}_i}{\partial\tilde{X}\,\partial y} - \Psi''_{00}(y)\frac{\partial\tilde{\psi}_i}{\partial\tilde{X}} = 0, \quad i = 1, 2, \ldots, 6. \tag{4.18}$$

From (4.9), it may be shown that $\mathrm{d}p/\mathrm{d}\tilde{x} \sim 1 + O(\tilde{\epsilon})$, and it follows that the equations for $\tilde{\psi}_i$ are independent of the pressure distribution in region $\tilde{\mathrm{B}}$ with solutions

$$\tilde{\psi}_i(\tilde{X}, y) = \frac{1}{\lambda_0}\tilde{B}_i(\tilde{X})\,\Psi'_{00}(y), \tag{4.19}$$

where the $\tilde{B}_i(\tilde{X})$ are arbitrary functions to be found.

Upon substitution of (4.19) into (4.17), the asymptotic behaviour of the stream function ψ for large values of y may be obtained using (4.6), and from (2.45) it is readily shown that the displacement function is of the form

$$A(x) = A_0(x_s) + \frac{\tilde{\epsilon}}{\lambda_0}(\log N)\,\tilde{B}_1(\tilde{X}) + \frac{\tilde{\epsilon}}{\lambda_0}(\log\log N)\,\tilde{B}_2(\tilde{X}) + \frac{\tilde{\epsilon}}{\lambda_0}\tilde{B}_3(\tilde{X}) + \ldots. \tag{4.20}$$

It follows from (2.43) that the expansion for pressure in region $\tilde{\mathrm{B}}$ is

$$p(x) = p_0(x_s) + N^{-1}(\log N)\lambda_0\tilde{X} + N^{-1}p_1(x_s) + N^{-1}\tilde{\epsilon}(\log N)\,\tilde{P}_1(\tilde{X}) + N^{-1}\tilde{\epsilon}(\log\log N)\,\tilde{P}_2(\tilde{X}) + N^{-1}\tilde{\epsilon}\tilde{P}_3(\tilde{X}) + \ldots, \tag{4.21}$$

where $\lambda_0 = p_0(x_s)$ and the interaction law reduces to

$$\frac{\mathrm{d}\tilde{P}_i}{\mathrm{d}\tilde{X}} = \frac{1}{\lambda_0}\frac{\mathrm{d}\tilde{B}_i}{\mathrm{d}\tilde{X}} \quad \text{for} \quad i = 1, 2, 3. \tag{4.22}$$

The thickness of layer $\bar{\mathrm{a}}$ (figure 9) decreases as $(-s)^{1/4}$ as $s\to 0^-$ and for layer $\tilde{\mathrm{A}}$, where $s = O(N^{-1}\log N)$, the characteristic normal variable $\tilde{Y}$ is

$$y = \epsilon^*\tilde{Y}, \quad \epsilon^* = N^{-1/4}\log^{1/4}N. \tag{4.23}$$

Using (4.2) and (4.10) written in terms of $\tilde{Y}$, it may be inferred that the form of the asymptotic expansion for ψ in region $\tilde{\mathrm{A}}$ is

$$\psi = \tfrac{1}{6}\epsilon^{*3}\lambda_0\tilde{Y}^3 + \epsilon^{*4}\tilde{\psi}_1^* + N^{-1}(\log\log N)\,\tilde{\psi}_2^* + N^{-1}\tilde{\psi}_3^* + \epsilon^{*5}\tilde{\psi}_4^* + \epsilon^* N^{-1}(\log\log N)\,\tilde{\psi}_5^* + \epsilon^* N^{-1}\tilde{\psi}_6^* + \ldots, \tag{4.24}$$

where the coefficients $\tilde{\psi}_i^*$ are functions of $\tilde{X}$ and $\tilde{Y}$ to be found. Substitution of (4.21) and (4.24) into (2.42) leads to equations for the $\tilde{\psi}_i^*$, the first three of which are

$$\tfrac{1}{2}\lambda_0\tilde{Y}^2\frac{\partial^2\tilde{\psi}_i^*}{\partial\tilde{X}\,\partial\tilde{Y}} - \lambda_0\tilde{Y}\frac{\partial\tilde{\psi}_i^*}{\partial\tilde{X}} = \frac{\partial^3\tilde{\psi}_i^*}{\partial\tilde{Y}^3}, \tag{4.25}$$

with the boundary conditions

$$\tilde{\psi}_i^* = \frac{\partial \tilde{\psi}_i^*}{\partial \tilde{Y}} = 0 \quad \text{at} \quad \tilde{Y} = 0, \quad \tilde{\psi}_i^* \to \tfrac{1}{2}\tilde{B}_i(\tilde{X})\,\tilde{Y}^2 + \ldots \quad \text{as} \quad \tilde{X} \to -\infty \quad \text{or} \quad \tilde{Y} \to +\infty. \tag{4.26a–c}$$

The solutions of (4.25) are

$$\tilde{\psi}_i^* = \tfrac{1}{2}\tilde{B}_i(\tilde{X})\,\tilde{Y}^2 \quad \text{for} \quad i = 1, 2, 3, \tag{4.27}$$

and it is easily shown that the arbitrary functions $\tilde{B}_i$ must have

$$\tilde{B}_1 \to a_0(-\tilde{X})^{1/2} - \tfrac{1}{4}\tilde{a}_1(-\tilde{X})^{-1/2} + \ldots, \quad \tilde{B}_2 \to \tfrac{1}{4}\tilde{a}_1(-\tilde{X})^{-1/2} + \ldots, \tag{4.28a, b}$$

$$\tilde{B}_3 \to \frac{\tilde{a}_1}{4}(-\tilde{X})^{-1/2}\log(-\tilde{X}) + a_1(-\tilde{X})^{-1/2} + \ldots, \tag{4.28c}$$

as $\tilde{X} \to -\infty$ in order to match the solution (4.2) and (4.10) in region $\bar{a}$. To determine the functions $\tilde{B}_1$, $\tilde{B}_2$ and $\tilde{B}_3$, the boundary-value problems for $\tilde{\psi}_4^*$, $\tilde{\psi}_5^*$, and $\tilde{\psi}_6^*$ must be considered (Smith & Daniels 1981), and it can be shown that

$$\tilde{B}_1 = a_0(\tilde{X}_s - \tilde{X})^{1/2}, \quad \tilde{B}_2 = \frac{\tilde{a}_1}{4}(\tilde{X}_s - \tilde{X})^{-1/2}, \tag{4.29a, b}$$

$$\tilde{B}_3 = \frac{\tilde{a}_1}{4}(\tilde{X}_s - \tilde{X})^{-1/2}\log(\tilde{X}_s - \tilde{X}) + a_1(\tilde{X}_s - \tilde{X})^{-1/2}. \tag{4.29c}$$

Here $\tilde{X}_s = -\tilde{a}_1/(2a_0)$ in order to satisfy (4.28), where X_s is positive in view of (4.13). It is evident that regions $\tilde{\mathrm{A}}$ and $\tilde{\mathrm{B}}$ simply serve to shift the singularity downstream to $\tilde{X}_s$ and that the pressure gradient does not influence the solution in either region $\tilde{\mathrm{A}}$ or $\tilde{\mathrm{B}}$ (cf. (4.25)). However, from (4.22) and (4.29) the last three terms in the pressure expansion (4.21) are now known, and it may be confirmed that the expansion becomes disordered when $\tilde{X}_s - \tilde{X} = O(\log^{-1} N)$.

Consequently, as shown in figure 9, a new viscous region A and an inviscid layer B centred on $\tilde{X} = \tilde{X}_s$ occur with an even shorter lengthscale, in order to accommodate the singular behaviour of the skin friction implied by (4.29). Defining a new streamwise variable by

$$x = x_s + N^{-1}\log N\tilde{X}_s + N^{-1}X_*, \tag{4.30}$$

and writing the solution (4.17) in region $\tilde{\mathrm{B}}$ in terms of X_* (using (4.27) and (4.29)), it may be verified that ψ must be expanded in region B as

$$\psi = \Psi_{00}(y) + N^{-1/2}\tilde{\Psi}_1^*(X_*, y) + \ldots. \tag{4.31}$$

The expansion for pressure in region B may be inferred by substitution of

$$\tilde{X} = \tilde{X}_s + \log^{-1} NX_*$$

in (4.21), and using (4.22) and (4.29), it follows that

$$p = p_0(x_s) + N^{-1}(\log N)\,\lambda_0\tilde{X}_s + N^{-1}[\lambda_0 X_* + p_1(x_s)] + N^{-3/2}(\log^{1/2} N)\,\tilde{P}_1(\tilde{X}_s) + N^{-3/2}P^*(X_*) + \ldots. \tag{4.32}$$

Substitution of (4.31) and (4.32) into the momentum equation (2.42) leads to

$$\tilde{\Psi}_1^* = \frac{1}{\lambda_0}B^*(X_*)\,\Psi_{00}'(y), \tag{4.33}$$

where $B^*(X_*)$ is an arbitrary function which must satisfy the condition

$$B^* \to a_0(-X_*)^{1/2} + \tfrac{1}{4}\tilde{a}_1(-X_*)^{-1/2}\log(-X_*) + a_1(-X_*)^{-1/2} + \ldots \quad \text{as} \quad X_* \to -\infty, \tag{4.34}$$

in order to match to the solution upstream in region $\tilde{\mathrm{B}}$. It follows from (4.31) that the displacement function is given by

$$A = A_0(x_s) + N^{-1/2}\frac{1}{\lambda_0}B^*(X_*) + \ldots, \tag{4.35}$$

and substitution of (4.32) and (4.35) into the interaction law (2.43) yields

$$\frac{\mathrm{d}P^*}{\mathrm{d}X_*} = \frac{1}{\lambda_0}\frac{\mathrm{d}B^*}{\mathrm{d}X_*}, \tag{4.36}$$

where $B^*(X_*)$ is still arbitrary.

The equation governing $B^*(X_*)$ is determined through consideration of the viscous layer A shown in figure 9. From (4.27) and (4.29), the thickness of region $\tilde{\mathrm{A}}$ is decreasing as $(\tilde{X}_s - \tilde{X})^{1/4}$ as $\tilde{X} \to \tilde{X}_s$; however, $(\tilde{X}_s - \tilde{X})$ becomes $O(\log^{-1} N)$ as region A is approached and, consequently, $\tilde{Y}$ is $O(\log^{-1/4} N)$. Therefore from (4.23) y is $O(N^{-1/4})$ in region A. Defining $y = N^{-1/4}Y_*$, substitution of $\tilde{Y} = Y_* \log^{-1/4} N$ in the expansion (4.24) in region $\tilde{\mathrm{A}}$ indicates that the asymptotic expansion for the stream function in region A has the form

$$\psi = N^{-3/4}\tfrac{1}{6}\lambda_0 Y_*^3 + N^{-1}\Psi_1^*(X_*, Y_*) + N^{-5/4}\Psi_2^*(X_*, Y_*) + \ldots. \tag{4.37}$$

It is readily shown that the solution for the first term is $\Psi_1^* = \frac{1}{2}B^*(X_*)\,Y_*^2$. The equation for Ψ_2^* contains the unknown pressure function $P^*(X_*)$ in the (4.32) and the solution satisfying the matching condition, $\Psi_2^* \to -a_0^2 Y_*^5/240$ as $X_* \to -\infty$, exists only if the skin-friction function B^* and P^* satisfy

$$2B^*\frac{\mathrm{d}B^*}{\mathrm{d}X_*} + a_0^2 = -(\tfrac{1}{2}\lambda_0)^{1/2}\frac{\Gamma(\frac{3}{4})}{\Gamma(\frac{5}{4})}\int_{-\infty}^{X_*}\frac{\mathrm{d}^2P^*/\mathrm{d}\xi^2}{(X_* - \xi)^{1/2}}\mathrm{d}\xi \tag{4.38}$$

(Stewartson 1970; Smith & Daniels 1981). Using the interaction law (4.36) and (4.13), it may be seen that (4.38) becomes

$$2B^*\frac{\mathrm{d}B^*}{\mathrm{d}X_*} + a_0^2 = \tilde{a}_1\int_{-\infty}^{X_*}\frac{\mathrm{d}^2B^*/\mathrm{d}\xi^2}{(X_* - \xi)^{1/2}}\mathrm{d}\xi. \tag{4.39}$$

Smith & Daniels (1981) showed that the solution of (4.39) satisfying (4.34) decreases with increasing X_* passing smoothly through zero at a positive value of X_*, denoted here as X_{*s}. Since the displacement function $B^*(X_*)$ is proportional to the skin friction, the boundary-layer solution therefore passes smoothly through separation at X_{*s} and a region of reversed flow occurs downstream of X_{*s}. However, the solution then terminates at a subsequent location downstream, denoted X_{*0}, where a more severe singularity develops with

$$B^* \to \tilde{a}_1(X_{*0} - X_*)^{-1/2} \quad \text{as} \quad X_* \to X_{*0}. \tag{4.40}$$

This behaviour implies a strengthening region of reversed flow and indicates that another nonlinear region, centred on X_{*0} and having a still shorter streamwise scale, must be considered in order to remove the singularity.

From (4.40), the second term in expansion (4.37) becomes comparable to the first in a new inner zone denoted as A′ in figure 9 where $Y_* = O(N^{-1/12})$ and

$$X_* - X_{*0} = O(N^{-1/3}).$$

New scaled variables in A′ are defined by

$$x = x_s + N^{-1}\log N\tilde{X}_s + N^{-1}X_{*0} + N^{-4/3}\lambda_0^{-5/3}X, \quad y = N^{-1/3}\lambda_0^{-2/3}Y, \quad (4.41a, b)$$

where the factors of λ_0 have been introduced for convenience. In the inviscid region B′ (figure 9), the characteristic variables are X and y and the expansions for stream function and pressure are

$$\psi = \Psi_{00}(y) + N^{-1/3}\lambda_0^{-2/3}B(x)\,\Psi'_{00} + \ldots, \quad (4.42)$$

$$p = p_0(x_s) + N^{-1}(\log N)\lambda_0\tilde{X}_s + N^{-1}\{p_1(x_s) + \lambda_0 X_{*0}\} + N^{-4/3}\lambda_0^{-2/3}P(X) + \ldots, \quad (4.43)$$

and in order to match the solution in region B

$$B(X) \to \tilde{a}_1(-X)^{-1/2} + \ldots, \quad P(X) \to X + \lambda_0^{1/2}\tilde{a}_1(-X)^{-1/2} + \ldots \quad \text{as} \quad X \to -\infty. \quad (4.44a, b)$$

The interaction law (2.43) gives

$$\frac{dP}{dX} = 1 + \frac{dB}{dX}. \quad (4.45)$$

In the inner region A′, the stream-function expansion is of the form

$$\psi = N^{-1}\lambda_0^{-1}\Psi(X, Y) + \ldots, \quad (4.46)$$

and substitution in (2.42) yields the following inner problem:

$$\frac{\partial\Psi}{\partial Y}\frac{\partial^2\Psi}{\partial X\partial Y} - \frac{\partial\Psi}{\partial X}\frac{\partial^2\Psi}{\partial Y^2} = -\frac{dP}{dX} + \frac{\partial^3\Psi}{\partial Y^3}, \quad (4.47)$$

with the boundary conditions

$$\Psi = \frac{\partial\Psi}{\partial Y} = 0 \quad \text{at} \quad Y = 0; \quad \Psi \to \tfrac{1}{6}Y^3 + \tfrac{1}{2}B(X)\,Y^2 \ldots \quad \text{as} \quad Y \to \infty, \quad (4.48)$$

along with the interaction law

$$P(X) = B(X) + X, \quad (4.49)$$

which follows from (4.44b) and (4.45). Finally to match the upstream solution in region A

$$\Psi = \tfrac{1}{6}Y^3 + \tfrac{1}{2}\tilde{a}_1(-X)^{-1/2}Y^2 + \ldots \quad \text{as} \quad X \to -\infty. \quad (4.50)$$

Smith & Daniels (1981) obtained a numerical solution of the interaction problem (4.47)–(4.50) and showed that a smooth solution exists for all X. Downstream of the separation point as $X \to \infty$, an extended separation region forms near the body surface. Consequently in the present case, for a sufficiently high ramp angle, separation occurs on the flat surface (figure 1), and an extended region of reversed flow develops downstream toward the ramp.

5. Concluding remarks

During the first decade after the seminal studies of Neiland (1969) and Stewartson & Williams (1969) on supersonic boundary-layer separation, it was widely recognized that self-induced separation theory could be applied to a range of separation phenomena at high Reynolds numbers. This was supported by Stewartson's (1970) conclusion that classical Prandtl boundary-layer theory, which leads to the formation of Goldstein singularity at a point of zero skin friction, cannot be improved by introducing an inner interaction region near the singular point, for either subsonic or

supersonic external flow. Self-induced separation theory was subsequently applied to a great number of phenomena associated with the boundary-layer separation, including supersonic and subsonic separation on a smooth surface, separation near corners of a body contour, and separation induced by wall blowing or by a jump in surface temperature.

Subsequently, it was determined that there are at least two situations when self-induced separation theory cannot be applied. The first is in marginal separation which was first discovered in a study of short separation bubbles that form near the leading edge of a thin airfoil (Stewartson *et al.* 1982; Ruban 1982). In this case, classical boundary-layer theory does not lead to the formation of a Goldstein singularity but rather to a relatively weaker singularity at the point of zero skin friction. The solution may be continued downstream of the marginal separation point, and therefore the Prandtl theory holds almost everywhere, requiring improvement only in the vicinity of the singular point; an interaction between the boundary layer and external inviscid flow governs the formation and possible bursting of the separation region. Here, it has been shown that marginal separation theory also describes supercritical boundary-layer separation on a cold wall. The present problem provides the first example where a smooth transformation of marginal separation theory into self-induced separation theory occurs, taking place here as the ramp angle increases. It is worthwhile to note that Cassel (1993) has carried out a series of calculations for a compression ramp with $N = O(1)$ and finds solutions which blend smoothly with increasing N into the structure obtained in §3.

There is a second general case of boundary-layer separation, namely that described by Smith & Daniels (1981) and used in §4 of the present paper to describe subcritical boundary-layer separation on a cold wall. In the present problem, there appears to be no other way of constructing a theory of the separation process, except the classical hierarchical approach leading to a Goldstein singularity. At the same time, the appearance of this singularity does not automatically imply a failure of the theory. While the singularity cannot be removed if the usual 'subsonic' or 'supersonic' interaction law is utilized (Stewartson 1970), it has been shown that it may be removed in the subcritical boundary layer on a cold wall when a 'compensation'-type interaction law governs the flow behaviour in the inner interaction region. The numerical solutions obtained by Cassel (1993) for increasing N also support the theory developed in §4. A further study of this regime has recently been carried out by Zhikharev (1993).

Part of the work was completed while A.I.R. was visiting Lehigh University as a United Technologies Fellow. This work was supported in part by United Technologies Corporation and the Air Force Office of Scientific Research under Grant No. 49620-93-1-0130.

Appendix A

Here the solution in the main deck (region 2 in figure 2) is considered for the case of a cold wall ($g_w \ll 1$). Upon substitution of the expansions (2.19*e*) and (2.30) into the Navier–Stokes equations, it is easily shown the streamwise momentum and energy equations become

$$\tilde{R}_0 \tilde{U}_0 \frac{\partial \tilde{U}_1}{\partial x^*} + \tilde{R}_0 \tilde{V}_1 \frac{\mathrm{d}\tilde{U}_0}{\mathrm{d}Y} = -S^* \frac{\mathrm{d}p^*}{\mathrm{d}x^*}, \quad \tilde{R}_0 \tilde{U}_0 \frac{\partial \tilde{H}_1}{\partial x^*} + \tilde{R}_0 \tilde{V}_1 \frac{\mathrm{d}\tilde{H}_0}{\mathrm{d}Y} = S^* \tilde{U}_0 \frac{\mathrm{d}p^*}{\mathrm{d}x^*}. \quad \text{(A 1}a, b\text{)}$$

Here the parameter $S^* = \chi^{1/4} g_w^{-(n+1/2)}$ is assumed $O(1)$. The continuity equation is

$$\tilde{R}_0 \frac{\partial \tilde{U}_1}{\partial x^*} + \tilde{U}_0 \frac{\partial \tilde{R}_1}{\partial x^*} + \tilde{R}_0 \frac{\partial \tilde{V}_1}{\partial Y} + \tilde{V}_1 \frac{\mathrm{d}\tilde{R}_0}{\mathrm{d}Y} = 0, \tag{A 2}$$

and from the ideal-gas equation of state

$$\tilde{R}_0 \tilde{H}_0 = \frac{1}{\gamma - 1}, \quad \tilde{H}_0 \tilde{R}_1 + \tilde{H}_1 \tilde{R}_0 = \frac{\gamma}{\gamma - 1} S^* p^*. \tag{A 3a, b}$$

To solve this system, differentiate (A 3b) with respect to x^* and using (A 3a) and (A 1b) to eliminate $\partial \tilde{H}_1 / \partial x^*$, it may be shown that

$$\tilde{U}_0 \frac{\partial \tilde{R}_1}{\partial x^*} + \tilde{V}_1 \frac{\mathrm{d}\tilde{R}_0}{\mathrm{d}Y} = \tilde{U}_0 \tilde{R}_0 S^* \frac{\mathrm{d}p^*}{\mathrm{d}x^*}. \tag{A 4}$$

Thus the continuity equation (A 2) becomes

$$\frac{\partial \tilde{U}_1}{\partial x^*} + \frac{\partial \tilde{V}_1}{\partial Y} = -\tilde{U}_0 S^* \frac{\mathrm{d}p^*}{\mathrm{d}x^*}, \tag{A 5}$$

and upon substitution for $\partial \tilde{U}_1 / \partial x^*$ in (A 1a), it follows that

$$\frac{\partial \tilde{V}_1}{\partial Y} - \frac{\tilde{V}_1}{\tilde{U}_0} \frac{\mathrm{d}\tilde{U}_0}{\mathrm{d}Y} = S^* \tilde{U}_0 \frac{\mathrm{d}p^*}{\mathrm{d}x^*} \left\{ \frac{1}{\tilde{R}_0 \tilde{U}_0^2} - 1 \right\}. \tag{A 6}$$

In view of conditions (2.8) which are satisfied by $\tilde{U}_0$ and $\tilde{R}_0$, the right-hand side of (A 6) has an integrable singularity as $Y \to 0$ and the solution matching that in the intermediate layer is

$$\tilde{V}_1 = \tilde{U}_0 \left\{ -\frac{\mathrm{d}A^*}{\mathrm{d}x^*} + S^* \frac{\mathrm{d}p^*}{\mathrm{d}x^*} \int_0^Y \left\{ \frac{1}{\tilde{R}_0 \tilde{U}_0^2} - 1 \right\} \mathrm{d}Y \right\}. \tag{A 7}$$

To leading order $M_0^2 = \tilde{R}_0 \tilde{U}_0^2$, where $M_0(Y)$ is the local Mach number in the outer part of the boundary layer approaching the interaction region (region β in figure 2). Evaluation of (A 7) at the boundary-layer edge $Y = \delta_0$ leads to the result (2.31).

Appendix B

Here the relation of the work of Brown *et al.* (1990) to the present study will be described in terms of the notation used in this paper. Brown *et al.* (1990) identify the same three parameter ranges described in §2.4 with $N \ll 1$, $N = O(1)$, and $N \gg 1$, referring to each situation as subcritical, transcritical and supercritical, respectively. Here, the terminologies subcritical ($\mathscr{L} > 0$) and supercritical ($\mathscr{L} > 0$) are used to connote the sign of the integral $\mathscr{L}$ in (2.32) as in Neiland (1973). Brown *et al.* (1990) do not address the situation $\mathscr{L} > 0$, but do obtain numerical solutions for the supercritical case ($\mathscr{L} < 0$) for both $N = O(1)$ and $N \gg 1$. The present theory for large N does not agree with a calculated result of Brown *et al.* (1990) (their $\sigma \to \infty$) and here the reasons for the discrepancy are addressed. The relationship between the variables defined in (2.41) and those utilized by Brown *et al.* (1990) for the large-N formulation may be expressed as

$$x = N^{-3} \tilde{x}, \quad y = N^{-1} \tilde{y}, \quad (\psi, p, F, A) = N^{-2} (\tilde{\psi}, \tilde{p}, \tilde{F}, \tilde{A}). \tag{B 1}$$

It has been suggested by a referee that the variables with the tilde provide the appropriate description for the case $N \to \infty$, and here this suggestion will be pursued. First it is clear that for large N and finite $\tilde{x}$ and $\tilde{y}$, the original variables x and y are small. Thus $(\tilde{x}, \tilde{y})$ may be considered to describe 'inner region' variables while (x, y) describe an outer region. The form of the interaction problems (2.42)–(2.47) is not altered by the transformations (B 1) apart from: (i) the interaction law (2.43) which becomes

$$\frac{\mathrm{d}}{\mathrm{d}\tilde{x}}(\mathrm{sgn}(\mathscr{L})\tilde{p} + \tilde{F} - \tilde{A}) = 0 \quad \text{for} \quad N \to \infty \tag{B 2}$$

(as in Brown *et al.* (1990; their equation (2.72) for large σ); and (ii) the equation of the ramp, which is now

$$\tilde{F} = 0 \quad \text{for} \quad \tilde{x} < 0; \quad \tilde{F} = (\beta/N)\tilde{x} \quad \text{for} \quad \tilde{x} > 0. \tag{B 3}$$

It is evident from (B 3) that in the new variables the apparent ramp angle is β/N and for $\beta = O(1)$ is small as $N \to \infty$.

The analysis in §§3 and 4 is based on the assumption that β is $O(1)$, and in such situations, the solution of the 'inner' interaction problem with (B 2) and (B 3) may be expressed as a small perturbation form about the trivial solution $\tilde{u} = \tilde{y}$ according to

$$\tilde{\psi} = \tfrac{1}{2}\tilde{y}^2 + \frac{\beta}{N}\tilde{\psi}_1(\tilde{x}, \tilde{y}) + \ldots, \quad p = \frac{\beta}{N}\tilde{p}_1(\tilde{x}) + \ldots, \quad \tilde{A} = \frac{\beta}{N}\tilde{A}_1(\tilde{x}) + \ldots. \tag{B 4}$$

It is evident therefore that for $\beta = O(1)$, the 'inner' region is non-characteristic and nothing of interest happens here. On the other hand, the situation where β/N is $O(1)$ implies that the lower deck produces a stronger displacement effect, and this is essentially the case considered by Brown *et al.* (1990) for large N. However, in this situation, the 'inner' region described by the variables (B 1) is deeply embedded in the outer region described by the variables in (2.41). As discussed in §§3 and 4, two cases arise depending on the sign of the integral $\mathscr{L}$ in (2.32).

In the subcritical case $\mathscr{L} > 0$ and separation takes place upstream of the ramp corner on the flat surface. For finite β, the distance between the separation point and the ramp corner is finite on the scale of the 'outer' variable x but very large on the scale of the 'inner' variable $\tilde{x}$. For larger values of β, separation takes place at an increasing distance from the ramp corner and, consequently, the 'inner interaction' region proposed by the referee would appear to be surrounded by a region of recirculating flow.

For the supercritical case $\mathscr{L} < 0$ and separation takes place downstream of the ramp corner for β being $O(1)$. With increasing β, the separation point moves closer to the corner while the reattachment point moves farther downstream. Thus to carry out a calculation in the 'inner' region suggested by the referee, a downstream boundary condition would be required which would properly match to a semi-infinite recirculation region as $\tilde{x} \to \infty$. The formulation of Brown *et al.* (1990) pertains for $N = O(1)$ wherein separation is generally confined to the immediate vicinity of the ramp corner; however as Brown *et al.* (1990) have noted, their calculated pressure distributions for large N (large σ) do not reach a plateau level downstream of the corner. In contrast, recent numerical solutions obtained by Cassel (1993) exhibit a pressure plateau for all N and clearly show that with increasing N the separation moves out of the corner and up onto the ramp. Cassel's (1993) results confirm those of the present study which show that the streamwise scale of the interaction region expands as $N \to \infty$ and that new scalings are necessary.

REFERENCES

ADAMSON, T. C. & MESSITER, A. F. 1980 Analysis of two-dimensional interactions between shock waves and boundary layers. *Ann. Rev. Fluid Mech.* **12**, 103–138.

BROWN, S. N., CHENG, H. K. & LEE, C. J. 1990 Inviscid–viscous interaction on triple-deck scales in a hypersonic flow with strong wall cooling. *J. Fluid Mech.* **220**, 309–337.

BROWN, S. N. & STEWARTSON, K. 1983 On an integral equation of marginal separation. *SIAM J. Appl. Maths* **43**, 1119–1126.

CASSEL, K. 1993 The effect of interaction on boundary-layer separation and breakdown. PhD thesis, Dept. of Mechanical Engineering and Mechanics, Lehigh University.

CHAPMAN, D. R., KUEHN, D. M. & LARSON, H. K. 1958 Investigation of separated flows in supersonic and subsonic streams with emphasis on the effect of transition. *NACA Tech. Rep.* 1356, pp. 419–460.

GOLDSTEIN, S. 1948 On laminar boundary-layer flow near a position of separation. *Q. J. Mech. Appl. Maths* **1**, 43–69.

HARTREE, D. R. 1939 A solution of the laminar boundary-layer equation for retarded flow. *Aeronaut. Res. Coun. Rep. Memo.* 2426 (issued 1949).

HOWARTH, L. 1938 On the solution of the laminar boundary layer equations. *Proc. R. Soc. Lond.* A **164**, 547–579.

JENSEN, R., BURGGRAF, O. R. & RIZZETTA, D. P. 1975 Asymptotic solution for the supersonic viscous flow past a compression corner. In *Proc. 4th Intl Conf. on Numerical Methods in Fluid Dynamics* (ed. R. D. Richtmyer). Lecture Notes in Physics, vol. 35, pp. 218–224. Springer.

LAGERSTROM, P. A. 1975 Solutions of the Navier–Stokes equation at large Reynolds number. *SIAM J. Appl. Maths* **28**, 202–214.

LANDAU, L. D. & LIFSCHITZ, E. M. 1944 *Mechanics of Continuous Media.* Moscow: Gostechizdat (in Russian).

LIGHTHILL, M. J. 1953 On boundary layers and upstream influence. II. Supersonic flows without separation. *Proc. R. Soc. Lond.* A **217**, 1131, 478–507.

MESSITER, A. F. 1970 Boundary-layer flow near the trailing edge of a flat plate. *SIAM J. Appl. Maths* **18**, 241–257.

MESSITER, A. F. 1979 Boundary-layer separation. In *Proc. 8th US Natl Congr. Appl. Mech.*, pp. 157–179. Western Periodicals, North Hollywood, California.

MESSITER, A. F. 1983 Boundary-layer interaction theory. *Trans. ASME* E: *J. Appl. Mech.*, **50**, 1104–1113.

MESSITER, A. F., MATARRESE, M. D. & ADAMSON, T. C. 1991 Strip blowing from a wedge at hypersonic speeds. *AIAA Paper* 91-0032.

NEILAND, V. YA. 1969 On the theory of laminar boundary layer separation in supersonic flow. *Izv. Akad. Nauk SSSR, Mech. Zhid. Gaza* No. 4, 53–57.

NEILAND, V. YA. 1973 Peculiarities of boundary-layer separation on a cooled body and its interaction with a hypersonic flow. *Izv. Akad. Nauk SSSR, Mech. Zhid. Gaza* No. 6, 99–109.

NEILAND, V. YA. 1974 Asymptotic problems of the viscous supersonic flow theory. *TsAGI Trans.* No. 1529.

NEILAND, V. YA. 1981 Asymptotic theory for separation and interaction of a boundary layer with supersonic gas flow. *Adv. Mech.* **4**, 3–62.

NEILAND, V. YA. & SOKOLOV, L. A. 1975 On the asymptotic theory of incipient separation in compression ramp hypersonic flow on cooled body for a weak hypersonic interaction regime. *Uchen. Zap. TsAGI*, **6** No. 3, 25–34.

PEARSON, H., HOLLIDAY, J. B. & SMITH, S. F. 1958 A theory of the cylindrical ejector supersonic propelling nozzle. *J. Aeronaut. Soc.* **62**, 756–761.

PRANDTL, L. 1904 Über Flüssigkeitsbewegung bei sehr Kleiner Reiburg. *Verb. III Intern. Math. Kongr., Heidelberg*; *Leipzig*, pp. 484–491. Teubner.

RUBAN, A. I. 1978 Numerical solution of the asymptotic problem for unsteady laminar boundary separation in supersonic flow. *Zh. Vychiesl. Mat. & Mat. Phys.* **18** (5), 1253–1265.

RUBAN, A. I. 1981 Singular solution for boundary layer equations with continuous extension downstream of zero skin friction point. *Izv. Akad. Nauk SSSR, Mech. Zhid. Gaza* No. 6, 42–52.

RUBAN, A. I. 1982 Asymptotic theory for short separation bubbles on the leading edge of thin airfoil. *Izv. Akad. Nauk SSSR, Mech. Zhid. Gaza* No. 1, 42–51.

SMITH, F. T. 1982 On the high Reynolds number theory of laminar flows. *IMA J. Appl. Maths* **28**, 207–281.

SMITH, F. T., BRIGHTON, P. W. M., JACKSON, P. S. & HUNT, J. C. R. 1981 On boundary-layer flow past two-dimensional obstacles. *J. Fluid Mech.* **113**, 123–152.

SMITH, F. T. & DANIELS, P. G. 1981 Removal of Goldstein's singularity at separation in flow past obstacles in wall layers. *J. Fluid Mech.* **110**, 1–37.

STEWARTSON, K. 1970 Is the singularity at separation removable? *J. Fluid Mech.* **44**, 347–364.

STEWARTSON, K. 1974 Multistructured boundary layers on flat plates and related bodies. *Adv. Appl. Mech.* **14**, 145–239.

STEWARTSON, K. 1981 D'Alembert's paradox. *SIAM Rev.* **23**, 308–343.

STEWARTSON, K., SMITH, F. T. & KAUPS, K. 1982 Marginal separation. *Stud. Appl. Maths* **67**, 45–61.

STEWARTSON, K. & WILLIAMS, P. G. 1969 Self-induced separation. *Proc. R. Soc. Lond.* A **312**, 181–206.

SYCHEV, V. V. 1972 On laminar separation. *Izv. Akad. Nauk SSSR, Mech. Zhid. Gaza* No. 3, 47–59.

SYCHEV, V. V., RUBAN, A. I., SYZHEV, VIK. V. & KOROLEV, G. L. 1987 *Asymptotic Theory for Separated Flows.* Moscow: Nauka.

TOWNEND, L. H. 1991 Research and design for hypersonic aircraft. *Phil. Trans. R. Soc. Lond.* A **335**, 201–224.

WALBERG, G. D. 1991 Hypersonic flight experience. *Phil. Trans. R. Soc. Lond.* A **335**, 91–119.

WERLE, M. J. & DAVIS, R. T. 1972 Incompressible laminar boundary layers on a parabola at angle of attack: a study of the separation point. *Trans. ASME* E: *J. Appl. Mech.* **39**, 7–12.

ZHIKHAREV, C. N. 1993 Separation phenomenon in hypersonic flow with strong wall cooling: subcritical regime. *Theoret. Comput. Fluid Dyn.* **4**, 209–226.